Review article: Using spaceborne lidar for snow depth retrievals: Recent findings and utility for ~~global~~ hydrologic applications

Zachary Fair[1,2], Carrie Vuyovich[1], Thomas Neumann[3], Justin Pflug[1,2], David Shean[4], Ellyn M. Enderlin[5], Karina Zikan[5], Hannah Besso[4], Jessica Lundquist[4], Cesar Deschamps-Berger[6], and Désirée Treichler[7]

[1]Hydrological Sciences Laboratory, NASA Goddard Space Flight Center, Greenbelt, MD, USA
[2]Earth System Science Interdisciplinary Center, University of Maryland, College Park, MD, USA
[3]Earth Sciences Division, NASA Goddard Space Flight Center, Greenbelt, MD, USA
[4]University of Washington, Seattle, WA, USA
[5]Department of Geosciences, Boise State University, Boise, ID, USA
[6]Pyrenean Institute of Ecology-CSIC, Avda Montañana 1005, Zaragoza 50.059. Spain
[7]Department of Geosciences, University of Oslo, Oslo, Norway

Correspondence: Zachary Fair (zachary.fair@nasa.gov)

Abstract. Lidar is an effective tool to measure snow depth over key watersheds across the United States. Lidar-derived snow depth observations from airborne platforms have demonstrated centimeter-level accuracy at high spatial resolution. However, ground-based and airborne lidar surveys are costly and limited in space and time. In recent years, there has been an emerging interest in using spaceborne lidar to estimate snow depth. Preliminary results from spaceborne lidar altimeters such as the NASA Ice, Cloud, and Land Elevation Satellite-2 (ICESat-2) can provide routine snow depth retrievals over watersheds, though further research on accuracy, coverage, and operational potential is needed. In this review, we outline the current status of research using spaceborne lidar to derive snow depth. We focus on the currently operational ICESat-2 mission, with a summary of snow observations gathered from previous studies. An example snow depth retrieval using ICESat-2 is also given over the Alaskan tundra. We also outline best practices for spaceborne lidar snow depth retrieval, based on findings from recent studies. We conclude with a discussion of ongoing challenges for spaceborne lidar, with suggestions for future studies and requirements for future mission concepts.

1 Introduction

Seasonal snow is a critical factor in Earth's climatological, ecological, and hydrological processes. Annually, seasonal snow covers a maximum extent of approximately 36% of the Earth's Northern Hemisphere (Estilow et al., 2015; Wrzesien et al., 2019), reflecting a significant portion of the incoming solar radiation and helping to cool the planet. Snow plays an integral role in the well-being of many high-latitude wildlife species and ecosystems, including the boreal forest, the largest terrestrial ecosystem (Boelman et al., 2019; Reinking et al., 2022). Melt water from seasonal snow accounts for approximately one-sixth of the world's freshwater supply and supports numerous hydrologic applications including hydropower, agriculture, and recreation (Barnett et al., 2005; Li et al., 2017). For these reasons, snow is listed as a future research need in a recent report by the Intergovernmental Panel on Climate Change (IPCC, 2022). Snow water equivalent (SWE) and depth are also identified

as Essential Climate Variables needed to better understand our changing climate by the Global Climate Observing System Implementation Plan (GCOS, 2022) and the 2017 Decadal Survey for earth science (NASEM, 2018).

As snow is highly variable over space and time (Sturm et al., 2010), it is especially important to capture SWE heterogeneity at basin-wide scales to accurately reproduce observed snowmelt, runoff, and streamflow in models (Brauchli et al., 2017; DeBeer and Pomeroy, 2017; Kiewiet et al., 2022). Frequent, high-resolution, spatially-distributed observations are needed to characterize this important component of the water and energy cycle. The observational requirements for SWE and snow depth stated in the GCOS Implementation Plan and the 2017 Decadal Survey suggest a spatial resolution of 500 m to 1 km, with higher resolution (100 m) needed in the mountains. Additional requirements include a temporal frequency of 1-5 days and an accuracy of 10-20%. While many

Many properties of snow are currently observable globally by satellites, including snow extent and albedo, we currently. Spaceborne technologies, notably multispectral imagers, have been most successful at mapping snow cover on the global scale. Currently, methods exist for mapping snow cover with the Landsat collection (??), Sentinel-2 (?), the Moderate Resolution Imaging Spectroradiometer (MODIS; Hall et al., 2002), and the Visible Infrared Imaging Radiometer Suite (VIIRS; Riggs et al., 2017). Methods also exist for retrieving the albedo and optical grain size of snow using MODIS and Sentinel-3 (??). Retrieval methods for snow depth and SWE are documented for sensors such as the Advanced Microwave Scanning Radiometer 2 (AMSR-2; ?) and Sentinel-1A (?). While these approaches offer valuable snow information at global and regional scales, they are challenged by multiple factors, including snow conditions (e.g., dry, wet, deep, or shallow snow), vegetation, and topography. Because of these challenges, we lack information about snow depth and SWE at the recommended scales needed to inform climate and water resource applications.

Recent studies have shown that it is possible to measure snow depth and fill gaps in global snow measurement capabilities from space using lidar altimetry. This is an appealing alternative to in-situ and airborne lidar methods because of its potential for global-scale observations. Spaceborne lidar derives snow depth using methods established with airborne lidar, including differential altimetry, and unique methods (Section 4). Spaceborne lidar altimeters, such as the Ice, Cloud, and Land Elevation Satellite-2 (ICESat-2; Markus et al., 2017) and the Global Ecosystem Dynamics Investigation (GEDI; Dubayah et al., 2020), provide accurate elevation observations, with centimeter-level accuracy for ICESat-2 over ice sheets and decimeter-level accuracy for both GEDI and ICESat-2 over forests (Adam et al., 2020; Brunt et al., 2021). Although current spaceborne platforms have relatively long revisit times and coarse across-track sampling, satellite altimetry could theoretically be used for routine measurements of snow depth over key watersheds, such as the Tuolumne River Basin in California, USA or the European Alps.

In this paper, we review the current status of research using spaceborne lidar, and evaluate its potential to derive snow depth to meet the research and operational needs of the hydrology community. Our discussion to accurately derive SWE. Our review is based on an extensive literature search using SciSpace, Web of Science, and research previously published by the authors. Based on our literature search, we determined that existing research on the subject concentrates on the currently operational ICESat-2 mission. We summarize published studies and present a case study over the tundra of Alaska to demonstrate accuracy and uncertainty estimates for several current methods. We also document challenges for current measurement approaches, with suggestions for future studies. We focus on terrestrial snow in this paper, but we acknowledge that snow depth retrievals have

also been attempted over land ice (Enderlin et al., 2022; Hu et al., 2022b; Lu et al., 2022) and sea ice (Hu et al., 2022b; Kwok et al., 2020; Lu et al., 2022). Snow depth measurements over ice masses have different challenges that are outside the scope of this review.

2 ~~Basic Lidar Principles~~

60 ~~Current~~

2 Spaceborne Lidar Missions

Spaceborne lidar systems follow similar principles to their airborne and ground-based counterparts. A detailed review of airborne and ground-based lidar is provided by (Deems et al., 2013) for interested readers. For a given instrument, key observation parameters include the footprint size, along-track resolution, and across-track resolution. A graphic outlining these terms is

65 shown in Figure 1. The footprint size represents the diameter of individual laser pulses at the surface. The footprint size is typically small - for instance, ICESat-2 has a footprint size of 11 m. Along-track resolution is determined by the pulse repetition rate of the instrument, and it defines the spacing between consecutive observations along the satellite track. For example, the base-level ICESat-2 product has an along-track resolution of 0.7 m. Across-track resolution describes effective width of a lidar swath, which can span kilometers for multi-beam systems like ICESat-2 and GEDI. However, these multi-beam

70 configurations create data gaps between individual beams within the swath.

A full list of known spaceborne lidar platforms and their operational periods may be found in Figure 2. The space-based lidar instruments ~~used to measure snow depth~~ listed have two primary measurement ~~modalities~~modality: waveform-based and photon-counting. Waveform lidar systems record the change in amplitude, or signal strength of the return, over time. The shape of the received waveform is sensitive to terrain characteristics such as surface roughness, which may cause centimeter-to-

75 decimeter levels of bias in the final elevation measurement (Dong and Chen, 2017). ~~Waveform-based spaceborne lidars include the original ICESat (Schutz et al., 2005) and the GEDI instrument (Dubayah et al., 2020).~~

Photon-counting lidar systems offer ~~a promising alternative for waveform lidar technology. Individual photons received by the instrument are time-tagged and geolocated~~ an alternative by time-tagging and geolocating received photons relative to a transmitted signal (Luthcke et al., 2021). Received photons are distinguished as signal or noise using automatic classification

80 algorithms that are based on either histograms of detected photons (Neumann et al., 2019) or more complex algorithms using iterative nearest-neighbor filters ~~(Neuenschwander and Magruder, 2019)~~ (Neuenschwander and Pitts, 2019) or photon-density approaches (Herzfeld et al., 2017). ~~Photon-counting lidars generally emit laser pulses at a higher rate than waveform-based platforms, which results in~~ While these systems provide improved along-track spatial resolution ~~and identification of fine-scale surface features. A drawback is that the~~ compared to waveform-based platforms, their lower transmitted energy ~~of these systems~~

85 ~~results in more attenuation through surfaces~~ results in greater attenuation through surface with low reflectance~~at the laser~~

Figure 1. Sample lidar swath (orange) to demonstrate along-track resolution, across-track resolution, and footprint size. In this example, the swath width (across-track resolution) is approximately 120 m, the footprint size is 10 m, and the along-track resolution is 50 m. Note that these values do not reflect any active or proposed spaceborne lidar mission, and they were arbitrarily selected for visualization purposes.

wavelength, which may limit measurement coverage. ~~At the time of writing, ICESat-2 currently is the only active civil-space photon-counting spaceborne lidar (Markus et al., 2017).~~

3 ~~Spaceborne Lidar Missions~~

~~A timeline of known spaceborne lidar missions for Earth Observation from 2000-present. Bars are colored by the primary wavelength(s) for each platform. The "Operational" section includes currently active missions, whereas the "Retired" section denotes missions that are no longer active. The "Future" section indicates missions that are expected to include lidar. GEDI was placed in temporary storage aboard the International Space Station from March 2023 to April 2024. The proposed EDGE mission concept has a notional 2 year duration, but it could be extended as GEDI and ICESat-2 have been.~~

~~Observed satellite laser altimetry maps of the Tuolumne River Basin, CA (highlighted in orange) using Landsat imagery. The blue lines represent the total coverage of each lidar satellite for a single winter (mid-December to mid-March) season: (a) ICESat in Winter 2008, (b) ICESat-2 in Winter 2022, and (c) GEDI in Winter 2022.~~

~~ICESat GEDI ICESat-2 DS17/GCOS Sensor Type Waveform Waveform Photon-counting — Wavelength 1064 nm 1064 nm 532 nm — Footprint diameter 70 m 25 m 11 m — Number of ground tracks 1 8 6 — Repeat time 2-3 times per year 3 days 91 days 3-5 days Max. Latitude 8651.68888(global) Along-track resolution 172 m 60 m 0.7 m 100 m Cross-track spacing — 600 m 3.3 km 100 m Instrument specifications for the spaceborne lidar platforms discussed in detail in this study. The recommendations given by the 2017 Decadal Survey (DS17) and GCOS are included for comparison.~~

In ~~this section~~ the following subsections, we describe the individual spaceborne lidar missions that have been used for snow studies. ~~A full list of known spaceborne lidar platforms and their operational periods may be found in Figure 1.~~ : ICESat, GEDI, and ICESat-2. A summary of the technical specifications for each spaceborne lidar is given in Table 1. We recognize ~~here that the~~ retired and future missions shown in Figure 1 that include spaceborne lidar technology. The Cloud-Aerosol Lidar and Infrared Pathfinder Satellite Observations (CALIPSO) mission included the Cloud-Aerosol Lidar with Orthogonal Polarization (CALIOP) as part of its scientific payload (Winker et al., 2009). The CALIOP instrument used polarized lidar backscatter to generate vertical profiles of clouds and aerosols in the atmosphere. Similarly, the Cloud-Aerosol Transport System (CATS) was a lidar onboard the International Space Station with similar science objectives to CALIPSO (McGill et al., 2015). However, both CALIPSO and CATS lacked surface elevation data products, and along-track resolution at the surface was compromised in favor of fine vertical resolution. Because of these limitations, the only snow application for CALIPSO known by the authors is the blowing snow product (Palm et al., 2017), and CATS has no known snow applications. Hence, we do not provide further discussion on CALIPSO or CATS in this paper. The Earth Dynamics Geodetic Explorer (EDGE) and the Surface Topography and Vegetation (STV) mission concepts are proposed spaceborne platforms that may include lidar as part of their respective payloads. If launched, both missions would become operational in the 2030s (Figure 1). More information about these missions may be found in Section ~~7.5~~ 6.5.

	ICESat	GEDI	ICESat-2	DS17/GCOS
Sensor Type	Waveform	Waveform	Photon-counting	—
Wavelength	1064 nm	1064 nm	532 nm	—
Footprint diameter	70 m	25 m	11 m	—
Number of ground tracks	1	8	6	—
Repeat time	2-3 times per year	3 days	91 days	3-5 days
Max. Latitude	86°	51.6°	88°	88°(global)
Along-track resolution	172 m	60 m	0.7 m	100 m
Cross-track spacing	—	600 m	3.3 km	100 m

Table 1. Instrument specifications for the spaceborne lidar platforms discussed in detail in this study. The recommendations given by the 2017 Decadal Survey (DS17) and GCOS are included for comparison.

2.1 ICESat

The original ICESat mission was launched in early 2002 with the goal of measuring interannual changes in ice elevation. Its sole onboard instrument, the Geoscience Laser Altimeter System (GLAS), primarily operated at 1064 nm, but it also included a photon-counting-based 532 nm channel to detect clouds and aerosols. The laser fired at a rate of 40 Hz with a 70 m footprint, with each measurement separated by 170 m along-track (Schutz et al., 2005). ICESat was originally conceived to operate continuously, but an engineering flaw in the three lasers required a change in the operation of GLAS to maximize laser lifetime (Abshire et al., 2005). ICESat performed a total of 18 33-day campaigns before ceasing operations in late 2009 (https://nsidc.org/sites/default/files/laseroperationalperiods.pdf).

The main altimetry products from ICESat are the GLAS/ICESat Level-2 products (GLAH12-15). Of these, the Global Land Surface Altimetry product (GLAH14) is designed for land-based elevation observations, so it is the preferred ICESat product for calculating the difference in elevation between snow-on and snow-free conditions to infer snow depth (Treichler and Kääb, 2017). However, there is approximately 70 km cross-track spacing at the mid-latitudes as a consequence of the limited observation strategy, so the coverage of ICESat is notably less comprehensive than other platforms over mid-latitude watersheds (Figure 2a3a).

2.2 GEDI

The GEDI mission was designed to measure canopy height and structure from space (Dubayah et al., 2020). GEDI was launched and added to the International Space Station (ISS) in December 2018 with a planned operational period of 2 years. The instrument operated continuously until it was temporarily placed in storage in March 2023 and returned to service in April 2024. GEDI is a full waveform lidar with a 1064 nm wavelength, similar to ICESat. The structure of the received waveform is used to distinguish between the ground and the canopy, and changes in the waveform amplitude and shape relative to the transmit pulse are used to derive canopy metrics. The GEDI footprint is 25 m in diameter, with 60 m along-track sampling

Figure 2. A timeline of known spaceborne lidar missions for Earth Observation from 2000-present. Bars are colored by the primary wavelength(s) for each platform: orange for 1064 nm and green for 532 nm. The "Operational" section includes currently active missions, whereas the "Retired" section denotes missions that are no longer active. The "Future" section indicates missions that are expected to include lidar. GEDI was placed in temporary storage aboard the International Space Station from March 2023 to April 2024. The proposed EDGE mission concept has a notional 2 year duration, but it could be extended as GEDI and ICESat-2 have been.

from 8 beams that are spaced 600 m apart in the cross-track direction (https://gedi.umd.edu). The GEDI product relevant for snow depth is the Level-2A product, which provides along-track ground elevation and canopy height estimates. Coverage and sampling density is limited by the ISS orbit inclination of 51.6°, though dense spatial coverage is available in the mid-latitudes (Figure 2c3c).

2.3 ICESat-2

The ICESat-2 mission was launched in September 2018 to continue measurements of surface height of ice sheets and sea ice, as begun by ICESat, as well as vegetation height. Like ICESat, it carries a single instrument, the Advanced Topographic
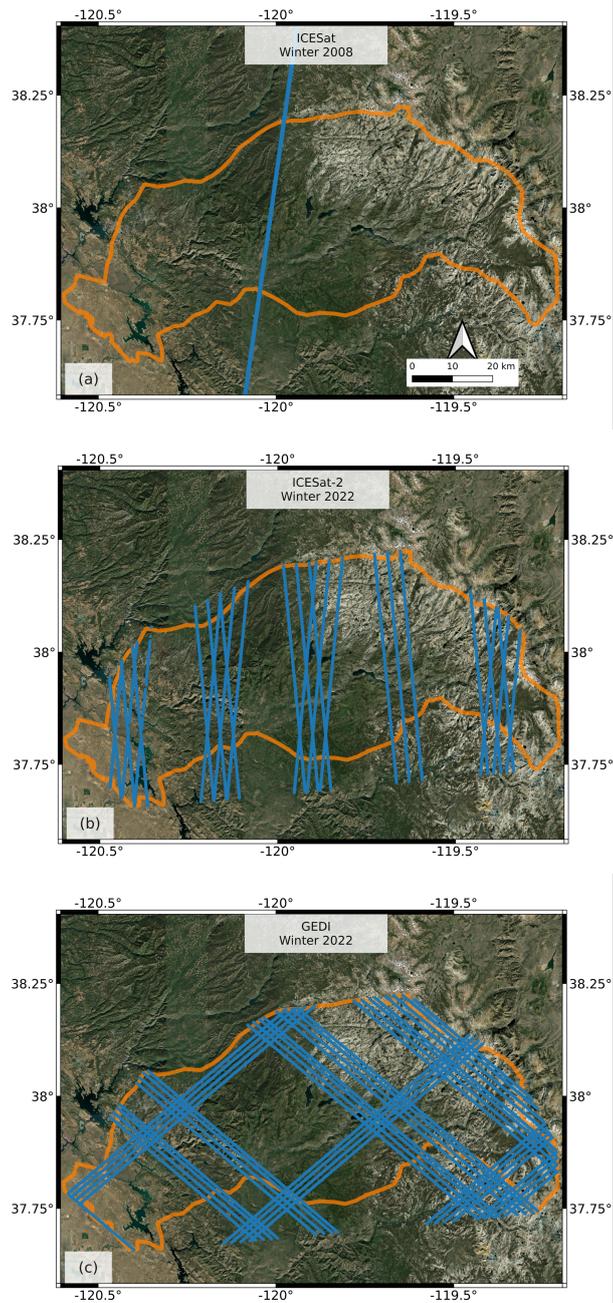
Figure 3. Observed satellite laser altimetry maps of the Tuolumne River Basin, CA (highlighted in orange), with Landsat imagery mosaics used as a basemap. The blue lines represent the total coverage of each lidar satellite for a single winter (mid-December to mid-March) season: (a) ICESat in Winter 2008, (b) ICESat-2 in Winter 2022, and (c) GEDI in Winter 2022.

145 Laser Altimeter System (ATLAS; Neumann et al., 2019). ATLAS is a photon-counting lidar that assigns a time and location (latitude and longitude) to each received photon. A single laser is split into 6 beams, with 3 beam pairs spaced by 3.3 km in the across-track direction and 90 m separation between beams within each pair. Each beam pair includes a strong beam and a weak beam to obtain sufficient coverage of high reflectivity (weak beam) and low reflectivity (strong beam) targets. The beams have an along-track sampling distance of 0.7 m, and each beam has a footprint of 11 m (Magruder et al., 2021), which

150 allows for significant footprint overlap. The satellite is in a polar orbit with an altitude of 500 km and a 91-day repeat cycle. The ICESat-2 orbit provides dense coverage near the poles that becomes sparser in the mid-latitudes (Figure 2b3b), with cross-track spacing of 2.5 km and 22 km at 80°N and 40°N, respectively. In the polar regions, data are collected along repeat ground tracks every 91-day cycle, while systematic and user-requested off-pointing at lower latitudes improve spatial coverage for vegetation mapping and for regions of interest. In the past year, the mission has pointed to prior data collections (repeat track pointing) to

155 enable snow applications.

ICESat-2 currently has 22 data products designed for analysis of ice sheets, vegetation, sea ice, and inland water. Of these products, three have been used in studies evaluating the potential for seasonal snow depth measurements: the Global Geolocated Photon Data product (ATL03); the Land Ice Elevation product (ATL06); and the Land, Water, and Vegetation Elevation product (ATL08). ATL03 is the base-level ICESat-2 product that is used to produce all higher-level products (Neumann et al., 2019). It

160 provides the highest in-track sampling at 0.7 m, but also has the least noise filtering applied. ATL06 estimates surface height by aggregating ATL03 photons into 40 m segments that overlap by 20 m (Smith et al., 2019). A windowed median is used to filter photons by quality and generate refined aggregations of surface height (Smith et al., 2018). The ATL08 product is designed to process ATL03 photons and discriminate between ground photons, noise, and several layers of tree canopies (Neuenschwander and Pitts, 2019). A median-based filtering algorithm known as the Differential, Regressive, and Gaussian Adaptive Nearest

165 Neighbor (DRAGANN) method is used to aggregate ground and canopy photons in 100 m segments with no overlap.

A recent development in the ICESat-2 community is SlideRule Earth, an open-source software package and an on-demand service to efficiently process ICESat-2 data in the cloud (Shean et al., 2023). In addition to facilitating standard ICESat-2 data product subsetting and delivery, SlideRule allows users to generate customizable ICESat-2 products using streamlined, parallel implementations of the ATL06 and ATL08 algorithms. Additional user controls allow for ATL03 photon filtering

170 based on signal confidence and the native ATL03, ATL08, and the Yet Another Photon Classifier (YAPC) photon classification approaches (Sutterley and Gibbons, 2021). It also includes support for efficient server-side sampling of large cloud-hosted DEM (e.g., ArcticDEM and REMA, 3DEP) archives, such as ArcticDEM, the Reference Elevation Model of Antarctica (REMA), and the 3-D Elevation Program (3DEP) (Porter et al., 2023; Stoker and Miller, 2022; Howat et al., 2022), as well as support for multiple GEDI products.

175 **3   Deriving Snow Depth from Lidar Products**

A list of existing studies using spaceborne lidar for snow applications is given in Table 2, with the locations or regions of interest shown in Figure 3. 4. The listed studies perform snow depth accuracy assessments for ICESat, GEDI (waveform-based) and
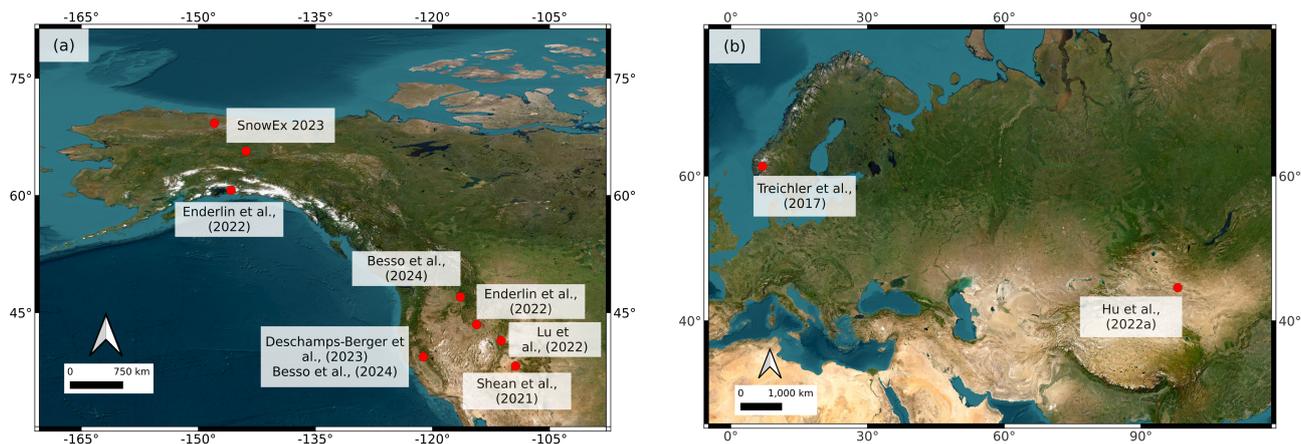
Figure 4. Maps of the study sites listed in Table 2, using a basemap derived from Landsat imagery. The maps zoom in to specific regions of interest, including the western United States and Alaska (a) and Europe and Asia (b). The relevant study is given for each location. The SnowEx 2023 field sites in Alaska are also shown, as extensive ICESat-2 tasking was performed for these sites and evaluation is ongoing. Lu et al. (2022) utilized ICESat-2 granules that spanned hundreds of kilometers, so only the midpoint of these granules is shown here.

ICESat-2 ~~, and GEDI~~ (photon-counting) data products, with evaluation of land cover classification and terrain characteristics. The NASA SnowEx campaigns in 2020, 2021, and 2023 also included targeted ICESat-2 off-pointing to collect data over field sites in Colorado (2020/2021) and Alaska (2023), with the goal of an assessment of ICESat-2 snow depths in mountainous terrain, boreal forests, and tundra (Vuyovich et al., 2022). Most of the featured studies derive snow depth using differential altimetry, though other methods have been proposed by the community for ICESat-2. When discussing the listed studies, bias refers to the difference, or residual, between spaceborne snow depths and validation depths, whereas uncertainty is a statistical range of depth values observed by a spaceborne platform. We also use the terms "accuracy" and "bias" interchangeably. We outline these approaches and findings from relevant scientific literature in the following subsections.

3.1 Differential Laser Altimetry

The most common method to derive snow depth from lidar is to compare two elevation datasets – one acquired when the surface was snow-free, and one acquired when the surface was snow-covered. Snow depth is assumed to be the elevation difference between the two datasets, with combined measurement uncertainty from both. This approach is known as "differential altimetry", and studies have applied this method to airborne/UAV lidar acquisitions (Deems et al., 2013; Painter et al., 2016; Harder et al., 2020; Jacobs et al., 2021) and terrestrial lidar acquisitions (Currier et al., 2019; Prokop, 2008; Revuelto et al., 2015) to achieve snow depth measurement accuracy of 6-17 cm, depending on the platform and study region. Figure ~~4~~ 5 provides a visual on the measurements needed to obtain snow depth via differential altimetry. The example in Figure ~~4~~ 5 is on sloped terrain with low-lying vegetation, which may introduce uncertainties to a depth retrieval (Section ~~6~~5).

Figure 5. A simple example showing how snow depth is calculated using differential altimetry, with ICESat-2 used as an analogue. A snow-off elevation measurement is first obtained (a), then a snow-on measurement is taken over the same location (b). The snow depth is taken as the difference between the two height measurements. Imagery is obtained from NASA SnowEx time-lapse cameras in Bonanza Creek Experimental Forest, Alaska on 14 October, 2022 (a) and 22 December, 2022 (b).

195   The differential method may also be used between spaceborne lidar observations and a reference snow-off DEM. The first known study to use spaceborne lidar for differential altimetry is Treichler and Kääb (2017), who used ICESat surface heights (GLAH14) and three reference DEMs to estimate snow depth in the forests of Norway. Preliminary work by Shean et al. (2021) found that GEDI snow depths had improved mid-latitude spatial coverage compared to ICESat and ICESat-2, but with larger biases and less temporal frequency. Subsequent work with spaceborne lidar has focused on ICESat-2. For instance,
200   Enderlin et al. (2022) used the ICESat-2 ATL06 and ATL08 products alongside airborne lidar and Worldview stereo imagery to derive snow depth over Wolverine Glacier, AK and Reynolds Creek Experimental Watershed, ID. The Tuolumne River Basin in California has been assessed by Deschamps-Berger et al. (2023) and Besso et al. (2024) using ATL06 and ATL06-SR (SlideRule) respectively, with the Airborne Snow Observatory (ASO) used as the primary DEM source. Besso et al. (2024) also examined Methow Valley, WA using SlideRule and airborne lidar from the USGS 3DEP program (Stoker and Miller, 2022).

205   ## 3.2   Other Methods

The differential method is the most common and consistent way to derive snow depth from lidar, but Hu et al. (2022b) devised a new technique that exploits time delay due to light penetration into the snowpack (see Section ~~6.4~~5.4) and ICESat-2 photon ~~distributions~~ counts to infer snow properties. Hu et al. (2022b) and Lu et al. (2022) deconvolved backscattered ICESat-2 photons that are reflected from the snow subsurface to derive path length distributions. These distributions are then used to
210   estimate snow depth, assuming that (i) terrestrial snow is a Lambertian surface and (ii) there is a sufficiently strong signal return. An uncertainty analysis was performed by Lu et al. (2022) for both studies. When compared to a daily 4 km resolution snow depth product, the authors found snow depths with a reported accuracy of 14 cm, with 23 cm in uncertainty. Hu et al. (2022b) also used ICESat-2 backscatter to estimate snow albedo and grain size, though the accuracy of these quantities was
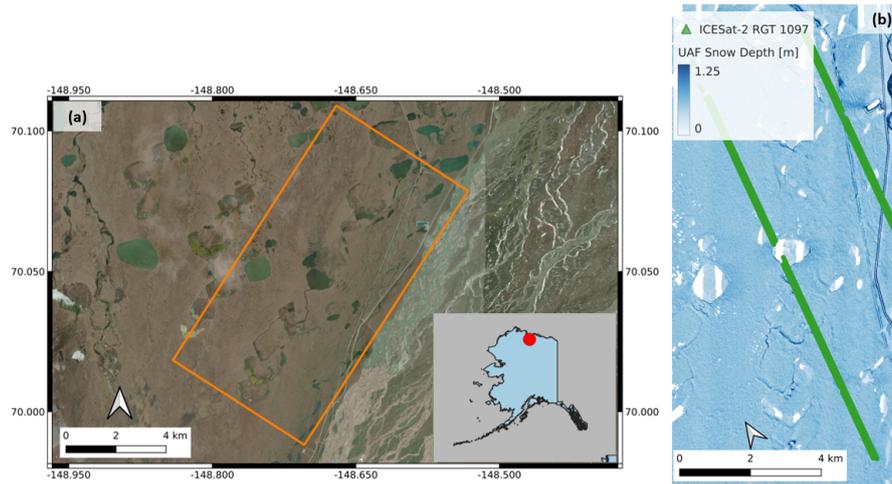
Figure 6. (a) Spatial domain of a SnowEx field site on the Alaskan coastal plain used for the retrieval example. The bottom right image shows the relative location of the site. (b) Snow depth product over the field site (orange box in (a)) as derived from UAF airborne lidar, with ICESat-2 RGT 1097 (March 4, 2022) given in green.

unclear due to a lack of validation data and coarse spatial resolution. Both studies encompassed a wide range of terrain features, including land ice, sea ice, and mountainous terrain.

It is possible to use repeat tracks of GEDI or ICESat-2 or "crossover" intersections from non-repeating tracks to perform differential altimetry measurements. Using this approach, Hu et al. (2022a) derived snow depth using intersecting ICESat-2 tracks over grasslands in Xinjiang, China, with a reported RMSE of 4 cm using ATL08. However, using cross-tracking spaceborne lidar paths consistently is difficult in the mid-latitudes due to infrequent repeat coverage, geolocation uncertainty in repeat tracks, and possible attenuation by clouds.

Based on the existing studies, ICESat-2 has shown the most promising results for spaceborne lidar snow depth measurements (Table 3), though studies using other platforms are limited. Generally, snow depth derived from ICESat-2 have an RMSE of up to 33 cm, as determined by the studies in Table 2. ICESat is shown to perform slightly worse, with an RMSE of 47 cm reported by Treichler and Kääb (2017). GEDI has the largest bias among the three lidar platforms, with an RMSE of 101 cm over Grand Mesa, CO (Shean et al., 2021). These platforms are also limited in their revisit frequency (ICESat) or their global coverage (GEDI). However, it must also be noted that the above assessments occur over different sites, so direct intercomparison is not possible. Because ICESat-2 has the most potential for snow depth applications, particularly over flat terrain, we will primarily focus on its measurement performance for the remainder of the paper.

4 ICESat-2 Case Study in Tundra Environment

Figure 7. ~~Snow depth comparisons between three~~ (a) Co-located ICESat-2 ~~products (ATL06, ATL08, ATL06-SR~~blue) and UAF ~~airborne~~ lidar (orange) surface elevations over the ~~ACP~~ example site in Northern Alaska. The ~~top row (a-c) shows along-track snow depth retrievals from~~ ICESat-2 ~~(GT2L)~~ data was obtained from March 4, 2022, and the UAF lidar ~~. The middle row (d-f)~~ data is ~~the scatter plot between the two retrieval methods~~from August 31, 2022 to emphasize elevation differences in snow-on and snow-off conditions. ~~The bottom row (g-i~~b) ~~is the distribution of~~ Snow depth ~~biases between~~ estimates from ICESat-2 and UAF ~~, with~~ lidar over the ~~median bias~~same track as ("Bias"a)~~and NMAD~~, with the UAF lidar depths originating from March 12, 2022. ICESat-2 snow depth is estimated as the difference between the two curves in ("spread"a)~~given for each~~.

~~To date, studies using differential altimetry from spaceborne lidar to derive snow depth have been assessed over forest, mountains, and glaciers. Tundra environments have not been evaluated~~ Previous sections outlined the basic principles and studies for snow depth retrievals ~~, despite the lack of vegetation and variable terrain that complicate retrievals. Here, we perform a case study over the Arctic Coastal Plain (ACP) of Alaska to fulfill two objectives:(i) to provide an example of along-track ICESat-2 snow depths, and (ii) to illustrate the potential value of~~ with spaceborne lidar. In this section, we provide a step-by-step example of the retrieval process over the Alaskan tundra. This section and the associated code sourced from the ICESat-2 ~~snow~~

~~depths over tundra environments~~2023 hackweek (https://icesat-2-2023.hackweek.io/tutorials/snow-depth/applications-tutorial-snow-depth. ?) enable interested readers to perform simple snow depth calculations with ICESat-2. These methods are also applicable to the original ICESat and GEDI, though different sites may require examination due to varying spatial coverage.

The Alaskan tundra serves as a useful ~~testbed for an accuracy assessment~~ example site for multiple reasons. First, the North

240 Slope of Alaska is at a higher latitude than previous studies, so there are a greater number of ICESat-2 tracks intersecting the region. Second, the ~~terrain over the Alaskan tundra is very flat , so errors due to slope or~~ flat terrain minimizes slope-related errors and issues with DEM co-registration~~are assumed to be negligible, particularly if a large-area aggregated comparison is performed (see Sections 6.1 and 6.2 for a discussion on terrain and DEM errors). Finally~~, thereby simplifying the retrieval process. Third, vegetation is limited to shrubs and tussocks. ~~Although~~ While low-lying vegetation and permafrost melt may

245 introduce centimeter-to-decimeter uncertainty to snow-off assessments (Section ~~6.3), similar~~ 5.3), comparable snow depths should be observed between airborne lidar and ~~spaceborne lidar, if~~ ICESat-2 when the snow-off lidar track is ~~flown~~ acquired within a year of the snow-on ICESat-2 track~~to account for permafrost changes~~.

~~The case study is performed using three~~ A snow depth retrieval with ICESat-2 requires snow-on surface elevation data, which is obtainable using either the icepyx (Scheick et al., 2023) or SlideRule Earth (Shean et al., 2023) Python packages.

250 The former provides access to pre-processed ICESat-2 ~~products: ATL06, ATL08, and ATL06-SR. The~~ ATL06 and ATL08 ~~data were accessed using icepyx, a Python tool that allows easy access of existing~~ that implement user-defined spatial and temporal boundaries, while the latter generates customized ICESat-2 data ~~products (Scheick et al., 2023). ATL06-SR data~~ from the ATL03 product. This example uses SlideRule Earth for its customization options, though the Zenodo code includes a data access routine for icepyx. SlideRule Earth was configured with ~~parameters that would differentiate from the ATL06~~

255 ~~and ATL08 products. The~~ a 20 m segment length ("len" in the code) and a 10 m along-track resolution ~~was set at 20 m rather than the default 40 m, and only high confidence signal photons were considered. ATL06-SR also allows the use of the ATL08 classification scheme, which we used to remove photons that did not originate from the ground.~~

~~The focus of this case study, the ACP site, is located near Prudhoe Bay on the northern coast (~~("res") within the region shown in Figure 6a. ATL03 photons within each segment were filtered for high-confidence photons ("cnf") originating from the surface

260 ("atl08_class"). For simplicity, data were obtained from a single reference ground track (RGT #1097) that overpassed the region on March 4, 2022. Figure ~~4a), and it encompasses a 75 km² tundra environment with little variation in topography. As part of the SnowEx campaign, a 1064 nm airborne lidar was flown by~~ 6b overlays the queried data on snow depth data from the University of Alaska ~~,~~ Fairbanks (UAF~~lidar)to obtain snow-on and snow-off data at 20 points per square meter and aggregated to 0.5 m resolution. Snow-off measurements were gathered on August 31, 2022 over the ACP site, and snow-on measurements~~

265 ~~were collected~~, Larsen, 2024).

The UAF lidar data were obtained over the region of interest on March 12, ~~2022. An ICESat-2 overpass took place on March 4,~~ 2022 ~~, with four of its beams overlapping the UAF lidar survey (Figure 4b). Although there is an eight-day offset between the~~ (snow-on~~acquisitions, snow accumulation between the two dates is assumed to be negligible based on reported precipitation data at the Deadhorse Airport weather station. Temperatures were well below freezing during the observation period, so we~~

~~also assume melt and sublimation were negligible. Wind speeds on and before the date of the ICESat-2 overpass were low (<10 kt), and they remained low up to the UAF lidar acquisitions.~~

~~The ICESat-2 snow depths were derived using differential altimetry between the ICESat-2 data products and snow-off data from the UAF lidar. Because the UAF data is provided as a gridded raster~~) and August 31, ~~rather than an along-track segment like ICESat-2, we utilized an interpolation scheme to sample UAF data along the~~ 2022 (snow-off), respectively. The data are provided in raster format at 0.5 m resolution, so they must be co-located with ICESat-2 ~~track. The UAF data were co-located to the~~ for proper analysis. A simple method to co-locate ICESat-2 ~~tracks using a bivariate~~ and UAF lidar is through a spline interpolant, which ~~uses available UAF snow-off and snow-on lidar data within a spatial domain to approximate surface elevation (snow-off) and snow depth (snow-on) as a function of spatial coordinates (i.e., latitude and longitude). In other words, the UAF lidar elevations and snow depths are sampled once every 20 m, 40 m, and 100 m along-track for ATL06-SR, ATL06, and ATL08, respectively, though the lidar data may not always be at the center of an~~ approximates surface elevation or snow depth such that:

$$h_{UAF} \propto f(x_{is2}, y_{is2}) \tag{1}$$

where h_{UAF} is UAF lidar surface elevation and x_{is2} and y_{is2} are the spatial coordinates along the ICESat-2 ~~segment. The~~ track. Figure 7a shows co-located UAF snow-off data with ICESat-2 ~~snow depth is then taken as the difference between~~ snow-on data. Although small, there is a clear positive difference in the ICESat-2 ~~snow-on surface elevation ($h_{is2,on}$) and the UAF snow-off elevation ($h_{\overline{uaf},off}$~~ elevations, which is interpreted as snow depth. If we calculate the difference between the co-located elevation products, we obtain ICESat-2 snow depth (d_{is2}):

$$\cancel{d_{is2} = \Delta h = h_{is2,on} - h_{uaf,off}}$$

$$d_{is2} = \Delta h = h_{is2,on} - h_{UAF,off} \tag{2}$$

~~Where Δh is the ICESat-2 snow depth in meters. The co-located UAF snow depths are then used as validation for the derived~~ where $h_{is2,on}$ is the snow-on ICESat-2 ~~depths. We used the median bias and normalized median absolute deviation (NMAD) for accuracy and uncertainty metrics, and we formally define both in Section 6.1~~ elevation and $h_{UAF,off}$ is the UAF lidar snow-off elevation (units of meters).

Figure ~~5 shows snow depth comparisons between ICESat-2 and UAF lidar over the coastal site. The number of snow depth data points differs between products due to the differing resolution of each: 845 depths for ATL06, 166 depths for ATL08, and 1546 depths for ATL06-SR. The different resolutions in 5a-c also illustrate variable levels of along-track variability in both ICESat-2 and UAF, with finer resolutions (ATL06 and ATL06-SR)showing greater spatial variability. However, the median snow depth is nearly the same between sampling resolutions: 48 cm for ATL06-SR and ATL06, and 50 cm for ATL08. Snow~~

15

~~depths derived from ICESat-2 show overall agreement with UAF across all three data products, as seen in 5a-5c. The scatter plots in 5d-f suggest that ICESat-2 somewhat underestimates depth relative to the airborne lidar , particularly at larger~~ 7b compares the calculated ICESat-2 snow depths to co-located UAF lidar depths. Despite the ~~underestimations, r^2 values are high for all three products: 0.88 for ATL06, 0.88 for ATL08, and 0.87 for ATL06-SR~~ simple co-location scheme, there is good agreement between the depth sources. The median bias and normalized median absolute deviation (NMAD~~) values are at the centimeter scale (3.7-4.8 cm for bias,~~, see Section 6.2) for the ICESat-2 depths are -4 cm and 5.7 ~~6.7 cmfor NMAD) for the three products, as seen in 5g-i. The biases and NMAD are comparable between products, which implies that all three products are well-suited to this environment~~cm, respectively, indicating high accuracy and low uncertainty in the derived depths.

~~Compared to previous studies for seasonal snow with different terrain and land cover types(Table 3), the biases and uncertainties observed in the tundra region are generally lower. The biases are also 10% of the total snow depth, which is within the desired accuracy defined by the Decadal Survey and GCOS (see Section 7.2). This supports the findings from previous studies, which found that spaceborne lidar snow depths improve in the absence of forests and sloped terrain (Besso et al., 2024; Deschamps-Berger et al., 2 . Lu et al. (2022) shows comparable biases to the case study over the Western United States, though more research will be needed to test their method over tundra environments relative to finer-scale measurements~~The process shown here is applicable to other watersheds, with ICESat and GEDI elevation data, and with other snow-off DEMs/DTMs. However, other environments may introduce factors affecting ICESat-2 retrieval accuracy and uncertainty, requiring users to experiment with different data products or SlideRule Earth configurations. The following sections provide greater detail on factors that may impact retrievals, as well as methods that may mitigate uncertainties.

5 Common Error Sources

The case study in Section ~~5~~ 4 demonstrates that accurate snow depth measurements in the tundra are possible to attain via ICESat-2. The studies in Table 2 also show that GEDI, ICESat, and ICESat-2 can retrieve snow depth over several land classes. However, snow depth accuracy and uncertainty differ between studies. The lidar platform and the retrieval method appear to have an influence, but accuracy and uncertainty also vary even between ICESat-2 studies using differential altimetry. In this section, we discuss possible sources of uncertainty for space-based lidar snow depth retrievals, including slope and terrain, vegetation, DEM source, and snowpack penetration. These error sources and the expected biases are summarized in Table 4.

5.1 Terrain Characteristics

Mountains have characteristic surface relief and roughness that can introduce horizontal and vertical uncertainty in lidar measurements (Deems et al., 2013). Complex topography spreads the footprint of a laser pulse non-uniformly, making precise geolocation of the received signal more difficult. Initial geolocation error is primarily related to instrument pointing errors that are exacerbated over sloped surfaces. Additional geolocation errors contribute directly to height errors as the tangent of the surface slope (Section 6.2). Pulse spreading also affects the return time of a received signal, adding uncertainty to surface

elevation estimates. It is therefore critical to identify ~~roughness- and~~ slope-based errors in both snow depth validation sources and in snow-free DEMs to quantify accuracy and uncertainty in lidar snow depth retrievals.

Several studies have quantified ~~slope-based errors~~ errors from surface roughness and slope in ICESat-2 surface heights and snow depths. Wang et al. (2019) found that ICESat-2 ATL03 snow-free data had sub-meter accuracy over flat surfaces, relative

335 to an airborne lidar over Alaska. Similar results were found in ICESat-2 ATL06 and ATL08 depths derived by Hu et al. (2022a), Enderlin et al. (2022), and Deschamps-Berger et al. (2023), with 4-20 cm in bias in all three studies at slopes < 10°. This error increases with ~~slope and propagates~~ surface roughness and slope, with Smith et al. (2019) finding <0.1 m accuracy in ATL06 over smooth surfaces and <1 m accuracy for rough surfaces. Errors in surface elevation also propagate to snow depths, with Enderlin et al. (2022) finding residuals and MAD values exceeding 1 m over slopes > 20°. The extent of slope-/aspect-based

340 uncertainty is noted by Nuth and Kääb (2011), with the study noting that elevation residuals exceeded 3 m when using satellite stereo imagery over slopes > 50° and forest covers > 40%. Besso et al., (2024) demonstrated that custom ATL06 processing of ATL03 photons (SlideRule) could be used to improve ICESat-2 snow depths over mountains and dense forest, with a maximum RMSE of 33 cm and a standard deviation of 105 cm obtained. Over slopes < 10°, the authors found a median residual of 5 cm that decreased to 1 cm at slopes 0-5°. The median residuals increased to 56-60 cm at slopes > 25°, which indicates general

345 improvement relative to previous studies.

5.2 DEM Accuracy and Co-Registration

The differential altimetry method to derive snow depth requires co-registration with a snow-off DEM or DTM, with different DEMs used in each of the studies highlighted above. However, DEM sources are frequently in different coordinate reference systems, and the reprojections needed prior to matching DEMs with lidar may produce geolocation uncertainties. Specifically,

350 vertical offsets between elevation data sets are related to the magnitude of the horizontal correction and the tangent of the terrain slope angle, so geolocation offsets are generally larger over steep slopes and rugged terrain. Because the accuracy of snow depth measurements depends on the accuracy of both the snow-off and snow-on altimetry, previous studies have calculated the most accurate spaceborne lidar snow depths using DEMs derived from airborne lidar. Deschamps-Berger et al. (2023) noted centimeter- to decimeter-scale biases over slopes below 50° even in dense forest cover when using an airborne

355 lidar DEM, while stereographic imagery performed similarly over flat, unvegetated sites but worse over steep slopes and dense forest.

The studies in Table 2 adopt a variety of strategies to align DEMs or digital terrain models (DTMs) with ICESat, ICESat-2, or GEDI. Although DEM/DTM geolocation offsets are generally small across the studies, the varied approaches highlight the lack of a consistent method to co-register spaceborne lidar with snow-off DEMs/DTMs. The use of a DEM with broad spatial

360 coverage, such as the 3DEP lidar or the Copernicus DEM, may enable spaceborne lidar snow studies on a regional to global scale. However, the choice of snow-free DEM/DTMs is also constrained by the need for a sufficiently high spatial resolution to resolve usable snow depths from ICESat-2. For example, Deschamps-Berger et al. (2023) found snow depth uncertainties greater than 3 m when using the Copernicus DEM, ~~and the authors excluded it from further analysis~~ compared to 0.6-1.16 m

uncertainties when using ASO or Pléiades. Besso et al. (2024) also found that the quality of the snow-off DEM was paramount,
365 to obtain meaningful snow depth aggregates.

5.3 Vegetation

Tree canopy has the potential to increase snow depth errors by decreasing the strength of lidar surface returns or absorbing
returns from snow underneath the canopy. Popescu et al. (2011) compared surface height measurements and canopy metrics be-
tween ICESat and airborne lidar data over the forests of eastern Texas. They found that ground height retrievals generally agreed
370 between the two platforms, though dense vegetation may spread the returned signal pulse from ICESat and generate a height
return within the tree canopy. Studies conducted by Feng et al. (2023), Neuenschwander et al. (2020), and Neuenschwander and
Magruder (2019) assessed the effects of tree canopies on ICESat-2 snow-on (October - April) and snow-off (May - September)
returns over boreal forests. The three studies found that the ATL08 product generally had terrain biases of -0.17 to +0.59 m over
regions of dense vegetation. Interestingly, surface height retrievals had lower uncertainty over snow-covered surfaces, which
375 was attributed to the high reflectance of signal photons of the optically-bright snow surface. Neuenschwander et al. (2020)
additionally found that ICESat-2 was more likely to detect the surface under low canopy conditions, particularly at canopy
cover <10%. We also expect that dense vegetation, such as bog understory within boreal forest environments, may be difficult
for lidar signals to penetrate, thereby increasing uncertainties. However, more research will be needed over high-latitude forests
to verify this claim.

380   Vegetative undergrowth, such as shrubs and tussocks, can introduce additional uncertainties in snow depth measurements.
Results by Ilangakoon et al. (2018), Simpson et al. (2017), and Spaete et al. (2011) suggest that undergrowth can cause
meter-level bias in snow-free DEMs, which can in turn produce negative snow depths in differential methods. During snow-on
conditions, regions of dense undergrowth will have strong snow depth variability at small spatial scales, introducing uncertainty
to lidar retrievals with comparatively large footprints (i.e., ICESat-2). For instance, results from Deschamps-Berger et al. (2023)
385 suggest that large errors in spaceborne lidar snow depths are associated with uncertainties in snow-free DEMs remain mostly
constant until forest cover densities over exceed 60%, with which large snow depth errors are observed. Besso et al. (2024)
found increased uncertainties over Methow Valley, WA relative to the Tuolumne River Basin, CA, with denser vegetation in the
valley thought to be the cause. Shrubland also proves a challenge for ground-based snow depth measurements (e.g., probing),
introducing uncertainty in the validation of airborne or spaceborne lidar snow depths.

390 ## 5.4 Lidar Penetration in Snow

Snow is weakly absorbing and highly reflective at wavelengths in the visible spectrum, resulting in a strong return signal over
snow. However, a laser pulse from ICESat-2 or another 532 nm lidar may also experience scattering within a snowpack. This
phenomenon, also known as "volumetric scattering", increases the time it takes for a signal to return to the detector. A modeling
study conducted by Smith et al. (2018) found that volumetric scattering could bias surface elevations from 532 nm lidar by
395 up to 50 cm when compared to 1064 nm lidar acquisitions. Observed results from Fair et al. (2024) constrain biases average
penetration depths (i.e., bias) in ICESat-2 data to 4-7 cm at the photon level, given optical grain sizes of 1000 μm or more.

However, these biases were quantified over snow and firn layers over a flat region of the Greenland Ice Sheet, and the authors speculated that it may be difficult to distinguish light penetration from other bias sources, such as topography or vegetation. Lu et al. (2022) tested their snow penetration algorithm over terrestrial snow and sea ice, and they speculated that it would be effective for snow depths up to 10 m. Snow reflectance at NIR wavelengths is much lower than that of green wavelengths, particularly as snow ages and melts. As a consequence, volumetric scattering is not a significant issue for NIR lidar (e.g., ICESat, GEDI, most airborne lidar), though the lower reflectance reduces return signal strength (Deems et al., 2013). The case study in Section 5 examines snow prior to the melt season, so snow grain size and altimetry bias are assumed to be small.

The penetration depth may also be used to estimate snow depth, with Lu et al. (2022) giving a maximum retrievable depth of 10 m using backscatter from within the snowpack. This maximum depth was determined using snow from late winter/early spring over mountainous snow and sea ice. However, more research will be needed to assess the limits of the method, as the authors generally found depths within 1 m over their study regions.

6 Suggestions for Future Studies and Applications to Hydrology

6.1 Uncertainties in Snow Depth Retrievals and SWE Estimates

Previous snow depth studies using ICESat-2 suggest that spaceborne lidar generally works well over flat surfaces in the absence of vegetation. Sloped terrain remains a significant challenge for snow depth retrievals, so barring improvements in the absolute geolocation accuracy of spaceborne lidar, development of processing and correction algorithms is essential for spaceborne snow depths over mountainous terrain. For instance, the SlideRule project offers ways to address issues related to vegetation and mountains, including configurable segment length and spatial step size, vegetation canopy treatment, and photon filtering (Besso et al., 2024). The choice of retrieval method may also affect accuracy. The signal convolution method by Hu et al. (2022b) and Lu et al. (2022) appears to have the best performance over the Western United States, with an RMSE of 14 cm and a standard deviation of 9.6 cm, though this is achieved by aggregating ICESat-2 observations to the resolution of a coarse reanalysis product (4 km).

Further uncertainties may be generated when converting lidar snow depths to SWE, ~~particularly if constant snow densities are used. Raleigh and Small (2017) show that uncertainty in snow density estimates is the largest source of error in SWE estimates when converting lidar~~ with snow density having a strong influence on SWE uncertainty. Bulk snow density is estimated across a domain using snow pit profiles (?) or empirical, statistical, or physically-based models (?Sturm et al., 2010; Painter et al., 2016). Snow pits provide direct measurements of snow density, though observations are subject to observer error, leading to SWE uncertainties of 10 cm (?). Simulated snow density varies by model, with Raleigh and Small (2017) finding an uncertainty range of 0.04-0.1 g cm^{-3}. The authors also found that snow density uncertainties strongly contributed to SWE errors when observed snow depths greater than 60 cm. Snow depth from these sources could be combined with ground-penetrating radar (GPR), physically-based and semi-empirical models, or in-situ snow densities to better estimate SWE (McGrath et al., 2022; Meehan et al., 2023; Webb et al., 2018).

6.2 Reported Accuracy Metrics

430 The studies outlined here generally use the mean or median difference to quantify biases in snow depths. However, the metrics used to quantify bias (accuracy) and uncertainty differ between studies (Table 3). Lu et al. (2022), Treichler and Kääb (2017), and Besso et al. (2024) also used the root mean square error (RMSE) to estimate snow depth errors relative to validation measurements. Uncertainty metrics are more varied across studies, including the standard deviation (Lu et al., 2022; Besso et al., 2024), interquartile range (Enderlin et al., 2022; Treichler and Kääb, 2017), the median absolute deviation (Enderlin

435 et al., 2022), and the normalized median absolute deviation (Deschamps-Berger et al., 2023). Each uncertainty metric assesses snow depth variability differently, so it is difficult to compare results between studies unless random error with a normal distribution is assumed.

Although the snow depth residuals in Figure 5 have a near-normal distribution, this is uncommon in other ICESat-2 snow depth studies, so robust statistical measures are needed. In our case study (Section 4.3), we selected the median residual and

440 normalized median absolute deviation (NMAD) to assess snow depth accuracy and uncertainty. These metrics can be computed using the following equations:

$$\delta d_i = d_{is2,i} - d_{uaf,i} \tag{3}$$

$$m_{\delta d} = median(\delta d) \tag{4}$$

$$NMAD = 1.4826 * median(|\delta d_i - m_{\delta d}|) \tag{5}$$

445 Where δd is the snow depth residual at point i, $m_{\delta d}$ is the median snow depth residual over all points, d_{is2} is the ICESat-2 snow depth, and d_{uaf} is the validation snow depth (UAF lidar in Section 4.3).

These metrics were used to minimize the influence of outliers in the data, which are otherwise common in fine-scale datasets such as ICESat-2 and the UAF lidar. The NMAD also has the advantage of being equivalent to the standard deviation if the underlying data has a normal distribution, provided a sufficiently large number of observations (Höhle and Höhle, 2009). Due

450 to the frequency of outliers, we recommend using the median bias and NMAD to quantify along-track spaceborne lidar snow depth error metrics in future studies. Estimating the percent error compared to total snow depth will also be useful to compare against 2017 Decadal Survey requirements.

6.3 Feasibility of Spaceborne Lidar to Support Snow Hydrology Science and Applications

The snow observation requirements, as reported by the 2017 Decadal Survey and the Global Observing System Essential

455 Climate Variables (GCOS ECVs), advocate for repeat global SWE measurements every 1-5 days with 10-20% accuracy (Table

4). Our literature review and case study demonstrate that ICESat-2 can provide high-resolution snow depths with centimeter-level accuracy under ideal conditions. Despite the shortcomings discussed in Section 6~~5~~, progress has been made on improving snow depth accuracy from spaceborne lidar. Kwon et al. (2021) conducted an observing system simulation experiment (OSSE) to determine the assimilated snow depth accuracy needed to improve snow models. It was found that an error threshold of 40 cm was needed to provide beneficial improvements to modeled SWE. This level of accuracy cannot be achieved through the current methods using ICESat and GEDI (Table 3). However, ICESat-2 is shown to perform within 40 cm of error, given (i) the local slope is less than 20° and (ii) an accurate, high-resolution snow-off DTM is used (Deschamps-Berger et al., 2023). Besso et al. (2024) also found that filtering ICESat-2 noise photons using SlideRule improved accuracy over complex terrain.

Spaceborne lidar is currently unable to fulfill the revisit times necessary to achieve global SWE observations every 1-5 days. Snow evolves throughout the season with accumulation events approximately every 5-7 days, or in strong episodic events (Pomeroy et al., 1998). Snow melt events occur over a period of days to months depending on the landscape and snow depth (Liston, 2004; Musselman et al., 2017). Capturing the timing of snow melt is especially critical to inform streamflow forecasting and water management (Anghileri et al., 2016; Gagliano et al., 2023). Spatial coverage of snow observations is also important for capturing the spatial variability of the snowpack. Currently, ICESat-2 direct repeats are every 91 days, though basin-scale repeats have shorter revisit times. GEDI has more frequent repeats (~3 days), but only over specific tracks. Kwon et al. (2021) showed that, with this limited coverage, there was minimal benefit when assimilating spaceborne lidar even with a hypothetical wide swath platform, though methods to extrapolate information from the lidar swath to a wider domain were not used.

A current limitation in achieving global snow depth observations from spaceborne lidar is the need for an accurate snow-off DEM when using the differencing approach, ideally from spaceborne lidar. Deschamps-Berger et al. (2023) showed that less than 2.5% of the Tuolumne Basin was covered by ICESat-2 during the snow-off season across three years. Additionally, no currently available global DEM product has demonstrated the ability to achieve accurate snow depths when combined with spaceborne snow-on lidar observations. Until a global DEM product with sufficient accuracy and resolution is available, the utility of spaceborne lidar for mid-latitude snow depth observations will be limited to locations with a high-quality snow-off DEM available.

An important consideration for future hydrologic applications is data latency. Current spaceborne lidar missions have a data latency on the order of months (a minimum of 1.5 months for ICESat-2, 4 months for GEDI), which hinders their utility for operational snow monitoring. To meet data needs for sea ice and vegetation applications, ICESat-2 provides expedited "quick look" data sets for several of its products. These quick look products are released three days after acquisition and downlink, though they do not include the pre-processing used to correct ICESat-2 orbital positioning and pointing. Otherwise, an ideal spaceborne lidar mission would include a low data latency with pre-processing applied, especially if regular monitoring of a watershed is desired.

6.4 Combining Spaceborne Lidar Data and Hydrologic Models

Some of the limitations in snow depth retrievals from spaceborne lidar may be overcome with hydrologic models and reanalysis products, in particular the limited coverage and repeat times. ~~Previous~~ Initiatives such as the Earth System Model-Snow

Model Intercomparison Project (ESM-SnowMIP), the European Center for Medium-Range Weather Forecasts (ECMWF) operational snow analysis, and the GlobSnow model have performed assessments of snow observations and model outputs over the Northern Hemisphere (???). In addition, previous studies have demonstrated that assimilation of airborne lidar observations can improve modeled estimates of snow depth, density, and SWE (Hedrick et al., 2018; Margulis et al., 2019; Smyth et al., 2019). These studies show that the greatest model improvement comes from one high-quality map of snow depth near the peak snowpack, suggesting that within a model framework, temporally continuous satellite data may not be necessary. However, lidar platforms with large temporal gaps are unlikely to capture critical snow evolution periods, such as the time of peak snow. Due to the low spatial coverage of spaceborne lidar overpasses, snow depth derived from satellite altimetry will likely be most useful for modeling if the limited extents of snow depth observations are used to infer snow depth in adjacent pixels to correct models. Multiple approaches for this application exist, including multidimensional Kalman filters/smoothers (Alonso-González et al., 2023; Magnusson et al., 2014); statistical approaches like kriging (Collados-Lara et al., 2017); interannual snow depth, snow cover, and SWE persistence patterns (Pflug et al., 2022); and other machine learning approaches (Cui et al., 2023; Guidicelli et al., 2024; Liu et al., 2024). For any of these methods, snow depth observations over multiple elevation regimes, aspects, and land cover types would contain more information than repeat airborne lidar observations over a single region (Margulis et al., 2019), as they would capture the widest variability in snow depth, snow density, and snowpack state. Because precipitation biases are responsible for significant errors in snow models (Henn et al., 2018; Pflug et al., 2021; Smyth et al., 2020; Wayand et al., 2015), accurate lidar observations during peak SWE and prior to melt onset would be useful to correct over- or under-estimation of snow accumulation. For instance, Guidicelli et al. (2024) found that assimilation of snow depth from a single ICESat-2 track from the late accumulation season improved estimated peak snow amounts. Assimilation of spaceborne lidar snow depths would also be beneficial during the melting season, where radar-based retrievals are less effective.

Provided a snow-off DEM, an ICESat-2 track can theoretically be used alongside historic SWE data to determine SWE over a large watershed of length scale 1-10 km. Assuming that SWE values are spatially correlated (i.e. all SWE values are above or below spatial or temporal averages), the broader watershed domain can be updated with a single ICESat-2 track. Accurately transforming ICESat-2 snow depth measurements to usable SWE estimates will require snow density observations, quantification of measurment uncertainty, and correlations between location-specific depth and domain-wide depth. Additionally, ensemble-based data assimilation frameworks, such as those described above, are ideal to accurately assimilate ICESat-2 depths into models. Besso et al. (2024) demonstrate that the median snow depth has little bias in the Tuolumne Basin, so even infrequent ICESat-2 snow depths could be used to accurately infer SWE throughout the snow season (Margulis et al., 2019). These findings were supported by Mazzolini et al. (2024), who performed a data assimilation study to improve reanalysis-derived SWE measurements using ICESat-2 snow depths. The ICESat-2 community has made data processing tools and workflows readily available through multiple hackweeks (Arendt et al., 2020), so the modeling community can easily conduct further data assimilation studies using ICESat-2 data.

Current SWE reconstruction methods use a combination of hydrologic models and reanalyses such as the ECMWF Reanalysis v5 (ERA5) and Modern-Era Retrospective analysis for Research and Applications, v2 (MERRA-2), but this approach can

only be used after the water year has occurred. Additionally, hydrologic models are improving constantly, but biases due to both modeling and forcing errors have significant implications on estimates of snow water resources (Kim et al., 2021; Mudryk et al., 2023; Raleigh et al., 2015). In many regions with significant snowfall, these modeling errors are chiefly caused by precipitation biases (Henn et al., 2018; Hughes et al., 2020; Lundquist et al., 2015; Pflug et al., 2021). As a consequence, models experience divergence in simulated snow accumulation, in heat content, and in the timing of seasonal snowmelt onset and snow disap-

pearance. However, previous studies have also shown that there is often repeatability in snow patterns on an interannual scale ~~(Deems et al., 2008; Pflug et al., 2022, 2021; Pflug and Lundquist, 2020; Schirmer et al., 2011; Schirmer and Lehning, 2011; Sturm and W~~ (Deems et al., 2008; Pflug et al., 2022, 2021; Pflug and Lundquist, 2020; Schirmer et al., 2011; Schirmer and Lehning, 2011; Sturm and W , so consistent observations near times of peak SWE will ideally bias correct modeled snow estimates at larger spatial scales.

6.5 Future Satellite Laser Altimetry Missions

The discussion in this paper focuses on currently operational satellite missions, primarily the ICESat-2 mission. However, there are future spaceborne lidar altimetry missions that may provide additional opportunities for snow depth retrievals upon launch. The first such lidar mission is the proposed EDGE mission, which is a NASA Earth System Explorer concept that was selected for Phase A study in May 2024. EDGE proposes a swath-mapping lidar with <3m horizontal geolocation accuracy for low slopes (https://edge.ucsd.edu/instrument/). EDGE will be a major technological advancement over currently operational satellite altimetry missions, with 40 beams distributed across five 8-beam mini-swaths that offer dense sampling in both the along-track and across-track directions. While the EDGE concept has been optimized for terrestrial ecosystem structure and ice elevation measurements, EDGE will also offer precise seasonal snow depth measurements using the same methods outlined in earlier sections. EDGE will also offer improved canopy penetration compared to ICESat-2, and will capture the spatial variability of snow depth across multiple relevant spatial length scales. If selected for continued development, EDGE is slated to launch in ~2030.

A second mission concept with a proposed lidar payload is the Surface Topography and Vegetation (STV) mission, which was conceived as a set of priority targeted observables for incubation study by the 2017 Earth Science Decadal Survey. The initial STV Study Team report (Donnellan et al., 2021) identified seasonal snow depth as one of 5 priority observables. Candidate measurement strategies include some combination of lidar, radar, and stereo photogrammetry, with candidate architecture including both satellites and airborne platforms. Multiple next-generation satellite lidar concepts, such as the Concurrent Artificially-intelligent Spectrometry and Adaptive Lidar System (CASALS), are under consideration, with ongoing technology maturation efforts underway in advance of the upcoming 2027 Decadal Survey. A launch for an STV observable is targeted for the mid-2030s.

7 Conclusions

With recent trends in climate change, it is becoming increasingly important to monitor available freshwater sources. Snow is a vital freshwater source for billions of people across the globe, so methods to monitor snow water equivalent and snow depth

are needed. In-situ and airborne instruments provide high-quality measurements of snow depth and SWE at select watersheds, but spaceborne methods will be required to obtain routine observations at larger spatial scales. Spaceborne lidar also has the potential to play a role in an overall global snow observing strategy by providing high-resolution snow depth observations, par-

ticularly during the season when other snow remote sensing techniques struggle. Recent developments show that spaceborne lidar ~~provide~~ provides useful snow depth data in areas where the local slope is below 20° and bare earth DEMs/DTMs are available. Over regions with consistent winter snow cover, these constraints are consistent with the Arctic tundra or plateaus/valleys in mountainous regions. Models which can ~~assimilation~~ assimilate observations and fill gaps in space and time are critical to utilizing spaceborne lidar for hydrological applications, though the exact measurement requirements to add value still need to be determined. There are currently two spaceborne lidar technologies available for snow applications: GEDI and ICESat-2. Of the two platforms, ICESat-2 generally offers better accuracy, greater coverage of high-latitude sites, and more continuous spatial coverage. However, Besso et al. (2024) demonstrated that customized processing of ICESat-2 products using SlideRule will be important to minimize uncertainties across variable terrain and land cover types. We recommend using median depth and the normalized median absolute deviation (NMAD) when assessing snow depth accuracy and uncertainty to reduce the influence of outliers.

There remain a few science questions that we leave for future studies. First, global snow depth observations from spaceborne lidar will not be possible until an accurate, high-resolution, DEM over regions with seasonal snow is available. To improve accuracy, a greater understanding of the geolocation accuracy of reference DEMs, and how said accuracy changes over time, is needed. This limitation highlights the need for an open-access, high-resolution global DEM, as current DEMs are limited in total coverage (ArcticDEM) or in spatial resolution (Copernicus DEM). A greater understanding of acceptable spatial resolution for reference DEMs is also needed to capture spatial variability in snow depth. At a regional scale, snow-free acquisitions are infrequent, and there is a risk of significant landscape changes occurring between DEM acquisition and spaceborne lidar retrieval, particularly in areas with melting permafrost. Second, more research is needed to validate spaceborne lidar snow depths against in-situ and airborne methods. Airborne methods such as the ASO campaigns will provide valuable, high-resolution snow depths for assessment and monitoring of mid-latitude watersheds. In-situ validation will be especially important to characterize uncertainties due to vegetation, which may be difficult to quantify with airborne and other space-based methods. Finally, more research is needed to determine how much of a watershed or basin must be sampled to improve modeled estimates. Combining spaceborne lidar observations with physical and statistical models may help fill observational gaps in an overall global snow observing strategy.

Code and data availability. The code used for the case study in Section 4 may be found at the following Zenodo link: https://doi.org/10.5281/zenodo.13852 Alternatively, it may be found in a more interactive form on the ICESat-2 hackweek Github: https://icesat-2-2023.hackweek.io/tutorials/snow-depth/applications-tutorial-snow-depth.html. The UAF lidar data (Larsen, 2024) and the ATL06/ATL08 data products (Smith et al., 2019; Neuenschwander and Pitts, 2019) were obtained from the National Snow and Ice Data Center (NSIDC). Documentation and instructions

on using may be found in (Shean et al., 2023). The camera imagery in Figure 4 was obtained during the SnowEx 2023 campaigns, and is currently pending upload to NSIDC.

References

Abshire, J. B., Sun, X., Riris, H., Sirota, J. M., McGarry, J. F., Palm, S., Yi, D., and Liiva, P.: Geoscience Laser Altimeter System (GLAS) on the ICESat Mission: On-orbit measurement performance, Geophysical Research Letters, 32, https://doi.org/10.1029/2005GL024028, _eprint: https://onlinelibrary.wiley.com/doi/pdf/10.1029/2005GL024028, 2005.

Adam, M., Urbazaev, M., Dubois, C., and Schmullius, C.: Accuracy Assessment of GEDI Terrain Elevation and Canopy Height Estimates in European Temperate Forests: Influence of Environmental and Acquisition Parameters, Remote Sensing, 12, 3948, https://doi.org/10.3390/rs12233948, number: 23 Publisher: Multidisciplinary Digital Publishing Institute, 2020.

Alonso-González, E., Aalstad, K., Pirk, N., Mazzolini, M., Treichler, D., Leclercq, P., Westermann, S., López-Moreno, J. I., and Gascoin, S.: Spatio-temporal information propagation using sparse observations in hyper-resolution ensemble-based snow data assimilation, Hydrology and Earth System Sciences, 27, 4637–4659, https://doi.org/10.5194/hess-27-4637-2023, publisher: Copernicus GmbH, 2023.

Anghileri, D., Voisin, N., Castelletti, A., Pianosi, F., Nijssen, B., and Lettenmaier, D. P.: Value of long-term streamflow forecasts to reservoir operations for water supply in snow-dominated river catchments, Water Resources Research, 52, 4209–4225, https://doi.org/10.1002/2015WR017864, _eprint: https://onlinelibrary.wiley.com/doi/pdf/10.1002/2015WR017864, 2016.

Arendt, A., Scheick, J., Shean, D., Buckley, E., Grigsby, S., Haley, C., Heagy, L., Mohajerani, Y., Neumann, T., Nilsson, J., Markus, T., Paolo, F. S., Perez, F., Petty, A., Schweiger, A., Smith, B., Steiker, A., Alvis, S., Henderson, S., Holschuh, N., Liu, Z., and Sutterly, T.: 2020 ICESat-2 Hackweek Tutorials, https://doi.org/10.5281/zenodo.3966463, 2020.

Barnett, T. P., Adam, J. C., and Lettenmaier, D. P.: Potential impacts of a warming climate on water availability in snow-dominated regions, Nature, 438, 303–309, https://doi.org/10.1038/nature04141, number: 7066 Publisher: Nature Publishing Group, 2005.

Besso, H., Shean, D., and Lundquist, J. D.: Mountain snow depth retrievals from customized processing of ICESat-2 satellite laser altimetry, Remote Sensing of Environment, 300, 113 843, https://doi.org/10.1016/j.rse.2023.113843, 2024.

Boelman, N. T., Liston, G. E., Gurarie, E., Meddens, A. J. H., Mahoney, P. J., Kirchner, P. B., Bohrer, G., Brinkman, T. J., Cosgrove, C. L., Eitel, J. U. H., Hebblewhite, M., Kimball, J. S., LaPoint, S., Nolin, A. W., Pedersen, S. H., Prugh, L. R., Reinking, A. K., and Vierling, L. A.: Integrating snow science and wildlife ecology in Arctic-boreal North America, Environmental Research Letters, 14, 010 401, https://doi.org/10.1088/1748-9326/aaeec1, publisher: IOP Publishing, 2019.

Brauchli, T., Trujillo, E., Huwald, H., and Lehning, M.: Influence of Slope-Scale Snowmelt on Catchment Response Simulated With the Alpine3D Model, Water Resources Research, 53, 10 723–10 739, https://doi.org/10.1002/2017WR021278, 2017.

Brunt, K. M., Smith, B. E., Sutterley, T. C., Kurtz, N. T., and Neumann, T. A.: Comparisons of Satellite and Airborne Altimetry With Ground-Based Data From the Interior of the Antarctic Ice Sheet, Geophysical Research Letters, 48, e2020GL090 572, https://doi.org/10.1029/2020GL090572, _eprint: https://onlinelibrary.wiley.com/doi/pdf/10.1029/2020GL090572, 2021.

Collados-Lara, A.-J., Pardo-Igúzquiza, E., and Pulido-Velazquez, D.: Spatiotemporal estimation of snow depth using point data from snow stakes, digital terrain models, and satellite data, Hydrological Processes, 31, 1966–1982, https://doi.org/10.1002/hyp.11165, _eprint: https://onlinelibrary.wiley.com/doi/pdf/10.1002/hyp.11165, 2017.

Cui, G., Anderson, M., and Bales, R.: Mapping of snow water equivalent by a deep-learning model assimilating snow observations, Journal of Hydrology, 616, 128 835, https://doi.org/10.1016/j.jhydrol.2022.128835, 2023.

Currier, W. R., Pflug, J., Mazzotti, G., Jonas, T., Deems, J. S., Bormann, K. J., Painter, T. H., Hiemstra, C. A., Gelvin, A., Uhlmann, Z., Spaete, L., Glenn, N. F., and Lundquist, J. D.: Comparing Aerial Lidar Observations With Terrestrial Lidar and Snow-Probe Transects

From NASA's 2017 SnowEx Campaign, Water Resources Research, 55, 6285–6294, https://doi.org/10.1029/2018WR024533, _eprint: https://onlinelibrary.wiley.com/doi/pdf/10.1029/2018WR024533, 2019.

DeBeer, C. M. and Pomeroy, J. W.: Influence of snowpack and melt energy heterogeneity on snow cover depletion and snowmelt runoff simulation in a cold mountain environment, Journal of Hydrology, 553, 199–213, https://doi.org/10.1016/j.jhydrol.2017.07.051, 2017.

Deems, J. S., Fassnacht, S. R., and Elder, K. J.: Interannual Consistency in Fractal Snow Depth Patterns at Two Colorado Mountain Sites, Journal of Hydrometeorology, 9, 977–988, https://doi.org/10.1175/2008JHM901.1, publisher: American Meteorological Society Section: Journal of Hydrometeorology, 2008.

Deems, J. S., Painter, T. H., and Finnegan, D. C.: Lidar measurement of snow depth: a review, Journal of Glaciology, 59, 467–479, https://doi.org/10.3189/2013JoG12J154, publisher: Cambridge University Press, 2013.

Deschamps-Berger, C., Gascoin, S., Shean, D., Besso, H., Guiot, A., and López-Moreno, J. I.: Evaluation of snow depth retrievals from ICESat-2 using airborne laser-scanning data, The Cryosphere, 17, 2779–2792, https://doi.org/10.5194/tc-17-2779-2023, publisher: Copernicus GmbH, 2023.

Dong, P. and Chen, Q.: LiDAR Remote Sensing and Applications, CRC Press, Boca Raton, ISBN 978-1-351-23335-4, https://doi.org/10.4324/9781351233354, 2017.

Donnellan, A., Harding, D., Lundgren, P., Wessels, K., Gardner, A., Simard, M., Parrish, C., Jones, C., Lou, Y., Stoker, J., Ranson, K. J., Osmanoglu, B., Lavalle, M., Luthcke, S., Saatchi, S., and Treuhaft, R.: Observing Earth's Changing Surface Topography and Vegetation Structure: A Framework for the Decade, NASA Surface Topography and Vegetation Incubation Study, Tech. rep., NASA Jet Propulsion Laboratory, https://smd-cms.nasa.gov/wp-content/uploads/2023/06/STV_Study_Report_20210622.pdf, 2021.

Dubayah, R., Blair, J. B., Goetz, S., Fatoyinbo, L., Hansen, M., Healey, S., Hofton, M., Hurtt, G., Kellner, J., Luthcke, S., Armston, J., Tang, H., Duncanson, L., Hancock, S., Jantz, P., Marselis, S., Patterson, P. L., Qi, W., and Silva, C.: The Global Ecosystem Dynamics Investigation: High-resolution laser ranging of the Earth's forests and topography, Science of Remote Sensing, 1, 100 002, https://doi.org/10.1016/j.srs.2020.100002, 2020.

Enderlin, E. M., Elkin, C. M., Gendreau, M., Marshall, H. P., O'Neel, S., McNeil, C., Florentine, C., and Sass, L.: Uncertainty of ICESat-2 ATL06- and ATL08-derived snow depths for glacierized and vegetated mountain regions, Remote Sensing of Environment, 283, 113 307, https://doi.org/10.1016/j.rse.2022.113307, 2022.

Estilow, T. W., Young, A. H., and Robinson, D. A.: A long-term Northern Hemisphere snow cover extent data record for climate studies and monitoring, Earth System Science Data, 7, 137–142, https://doi.org/10.5194/essd-7-137-2015, publisher: Copernicus GmbH, 2015.

Fair, Z., Flanner, M., Neumann, T., Vuyovich, C., Smith, B., and Schneider, A.: Quantifying volumetric scattering bias in ICESat-2 and Operation IceBridge altimetry over Greenland firn and aged snow, AGU Earth and Space Science, 11, 2022EA002 479, https://doi.org/10.1029/2022EA002479, 2024.

Feng, T., Duncanson, L., Montesano, P., Hancock, S., Minor, D., Guenther, E., and Neuenschwander, A.: A systematic evaluation of multi-resolution ICESat-2 ATL08 terrain and canopy heights in boreal forests, Remote Sensing of Environment, 291, 113 570, https://doi.org/10.1016/j.rse.2023.113570, 2023.

Gagliano, E., Shean, D., Henderson, S., and Vanderwilt, S.: Capturing the Onset of Mountain Snowmelt Runoff Using Satellite Synthetic Aperture Radar, Geophysical Research Letters, 50, e2023GL105 303, https://doi.org/10.1029/2023GL105303, _eprint: https://onlinelibrary.wiley.com/doi/pdf/10.1029/2023GL105303, 2023.

GCOS: The 2022 GCOS ECVs Requirements (GCOS 245), https://library.wmo.int/records/item/58111-the-2022-gcos-ecvs-requirements-gcos-245, 2022.

27

Guidicelli, M., Aalstad, K., Treichler, D., and Salzmann, N.: A Combined Data Assimilation and Deep Learning Approach for Continuous Spatio-Temporal SWE Reconstruction from Sparse Ground Tracks, https://doi.org/https://doi.org/10.1016/j.hydroa.2024.100190, 2024.

Hall, D. K., Riggs, G. A., Salomonson, V. V., DiGirolamo, N. E., and Bayr, K. J.: MODIS snow-cover products, Remote Sensing of Environment, 83, 181–194, https://doi.org/10.1016/S0034-4257(02)00095-0, 2002.

Harder, P., Pomeroy, J. W., and Helgason, W. D.: Improving sub-canopy snow depth mapping with unmanned aerial vehicles: lidar versus structure-from-motion techniques, The Cryosphere, 14, 1919–1935, https://doi.org/10.5194/tc-14-1919-2020, publisher: Copernicus GmbH, 2020.

Hedrick, A. R., Marks, D., Havens, S., Robertson, M., Johnson, M., Sandusky, M., Marshall, H.-P., Kormos, P. R., Bormann, K. J., and Painter, T. H.: Direct Insertion of NASA Airborne Snow Observatory-Derived Snow Depth Time Series Into the iSnobal Energy Balance Snow Model, Water Resources Research, 54, 8045–8063, https://doi.org/10.1029/2018WR023190, _eprint: https://onlinelibrary.wiley.com/doi/pdf/10.1029/2018WR023190, 2018.

Henn, B., Painter, T. H., Bormann, K. J., McGurk, B., Flint, A. L., Flint, L. E., White, V., and Lundquist, J. D.: High-Elevation Evapotranspiration Estimates During Drought: Using Streamflow and NASA Airborne Snow Observatory SWE Observations to Close the Upper Tuolumne River Basin Water Balance, Water Resources Research, 54, 746–766, https://doi.org/10.1002/2017WR020473, _eprint: https://onlinelibrary.wiley.com/doi/pdf/10.1002/2017WR020473, 2018.

Herzfeld, U. C., Trantow, T. M., Harding, D., and Dabney, P. W.: Surface-Height Determination of Crevassed Glaciers—Mathematical Principles of an Autoadaptive Density-Dimension Algorithm and Validation Using ICESat-2 Simulator (SIMPL) Data, IEEE Transactions on Geoscience and Remote Sensing, 55, 1874–1896, https://doi.org/10.1109/TGRS.2016.2617323, conference Name: IEEE Transactions on Geoscience and Remote Sensing, 2017.

Howat, I., Porter, C., Noh, M.-J., Husby, E., Khuvis, S., Danish, E., Tomko, K., Gardiner, J., Negrete, A., Yadav, B., Klassen, J., Kelleher, C., Cloutier, M., Bakker, J., Enos, J., Arnold, G., Bauer, G., and Morin, P.: The Reference Elevation Model of Antarctica - Mosaics, Version 2, https://doi.org/10.7910/DVN/EBW8UC, 2022.

Hu, X., Hao, X., Wang, J., Huang, G., Li, H., and Yang, Q.: Can the Depth of Seasonal Snow be Estimated From ICESat-2 Products: A Case Investigation in Altay, Northwest China, IEEE Geoscience and Remote Sensing Letters, 19, 1–5, https://doi.org/10.1109/LGRS.2021.3078805, conference Name: IEEE Geoscience and Remote Sensing Letters, 2022a.

Hu, Y., Lu, X., Zeng, X., Stamnes, S. A., Neuman, T. A., Kurtz, N. T., Zhai, P., Gao, M., Sun, W., Xu, K., Liu, Z., Omar, A. H., Baize, R. R., Rogers, L. J., Mitchell, B. O., Stamnes, K., Huang, Y., Chen, N., Weimer, C., Lee, J., and Fair, Z.: Deriving Snow Depth From ICESat-2 Lidar Multiple Scattering Measurements, Frontiers in Remote Sensing, 3, https://doi.org/10.3389/frsen.2022.855159, 2022b.

Hughes, M., Lundquist, J. D., and Henn, B.: Dynamical downscaling improves upon gridded precipitation products in the Sierra Nevada, California, Climate Dynamics, 55, 111–129, https://doi.org/10.1007/s00382-017-3631-z, 2020.

Höhle, J. and Höhle, M.: Accuracy assessment of digital elevation models by means of robust statistical methods, ISPRS Journal of Photogrammetry and Remote Sensing, 64, 398–406, https://doi.org/10.1016/j.isprsjprs.2009.02.003, 2009.

Ilangakoon, N. T., Glenn, N. F., Dashti, H., Painter, T. H., Mikesell, T. D., Spaete, L. P., Mitchell, J. J., and Shannon, K.: Constraining plant functional types in a semi-arid ecosystem with waveform lidar, Remote Sensing of Environment, 209, 497–509, https://doi.org/10.1016/j.rse.2018.02.070, 2018.

IPCC: High Mountain Areas, in: The Ocean and Cryosphere in a Changing Climate: Special Report of the Intergovernmental Panel on Climate Change, edited by Intergovernmental Panel on Climate Change (IPCC), pp. 131–202, Cambridge University Press, Cambridge, ISBN 978-1-00-915796-4, https://doi.org/10.1017/9781009157964.004, 2022.

710 Jacobs, J. M., Hunsaker, A. G., Sullivan, F. B., Palace, M., Burakowski, E. A., Herrick, C., and Cho, E.: Snow depth mapping with un-piloted aerial system lidar observations: a case study in Durham, New Hampshire, United States, The Cryosphere, 15, 1485–1500, https://doi.org/10.5194/tc-15-1485-2021, publisher: Copernicus GmbH, 2021.

Kiewiet, L., Trujillo, E., Hedrick, A., Havens, S., Hale, K., Seyfried, M., Kampf, S., and Godsey, S. E.: Effects of spatial and temporal variability in surface water inputs on streamflow generation and cessation in the rain–snow transition zone, Hydrology and Earth System

715 Sciences, 26, 2779–2796, https://doi.org/10.5194/hess-26-2779-2022, 2022.

Kim, R. S., Kumar, S., Vuyovich, C., Houser, P., Lundquist, J., Mudryk, L., Durand, M., Barros, A., Kim, E. J., Forman, B. A., Gutmann, E. D., Wrzesien, M. L., Garnaud, C., Sandells, M., Marshall, H.-P., Cristea, N., Pflug, J. M., Johnston, J., Cao, Y., Mocko, D., and Wang, S.: Snow Ensemble Uncertainty Project (SEUP): quantification of snow water equivalent uncertainty across North America via ensemble land surface modeling, The Cryosphere, 15, 771–791, https://doi.org/10.5194/tc-15-771-2021, publisher: Copernicus GmbH, 2021.

720 Kwok, R., Kacimi, S., Webster, M., Kurtz, N., and Petty, A.: Arctic Snow Depth and Sea Ice Thickness From ICESat-2 and CryoSat-2 Free-boards: A First Examination, Journal of Geophysical Research: Oceans, 125, e2019JC016 008, https://doi.org/10.1029/2019JC016008, _eprint: https://onlinelibrary.wiley.com/doi/pdf/10.1029/2019JC016008, 2020.

Kwon, Y., Yoon, Y., Forman, B. A., Kumar, S. V., and Wang, L.: Quantifying the observational requirements of a space-borne LiDAR snow mission, Journal of Hydrology, 601, 126 709, https://doi.org/10.1016/j.jhydrol.2021.126709, 2021.

725 Larsen, C. F.: SnowEx23 Airborne Lidar-Derived 0.25M Snow Depth and Canopy Height, Version 1, https://doi.org/10.5067/BV4D8RRU1H7U, 2024.

Li, D., Wrzesien, M. L., Durand, M., Adam, J., and Lettenmaier, D. P.: How much runoff originates as snow in the western United States, and how will that change in the future?, Geophysical Research Letters, 44, 6163–6172, https://doi.org/10.1002/2017GL073551, _eprint: https://onlinelibrary.wiley.com/doi/pdf/10.1002/2017GL073551, 2017.

730 Liston, G. E.: Representing Subgrid Snow Cover Heterogeneities in Regional and Global Models, https://journals.ametsoc.org/view/journals/clim/17/6/1520-0442_2004_017_1381_rsschi_2.0.co_2.xml, section: Journal of Climate, 2004.

Liu, Z., Filhol, S., and Treichler, D.: Retrieving snow depth distribution by downscaling ERA5 Reanalysis with ICESat-2 laser altimetry, arXiv, https://doi.org/10.48550/arXiv.2410.17934, 2024.

Lu, X., Hu, Y., Zeng, X., Stamnes, S. A., Neuman, T. A., Kurtz, N. T., Yang, Y., Zhai, P.-W., Gao, M., Sun, W., Xu, K., Liu, Z.,

735 Omar, A. H., Baize, R. R., Rogers, L. J., Mitchell, B. O., Stamnes, K., Huang, Y., Chen, N., Weimer, C., Lee, J., and Fair, Z.: Deriving Snow Depth From ICESat-2 Lidar Multiple Scattering Measurements: Uncertainty Analyses, Frontiers in Remote Sensing, 3, https://doi.org/10.3389/frsen.2022.891481, 2022.

Lundquist, J. D., Hughes, M., Henn, B., Gutmann, E. D., Livneh, B., Dozier, J., and Neiman, P.: High-Elevation Precipitation Patterns: Using Snow Measurements to Assess Daily Gridded Datasets across the Sierra Nevada, California, Journal of Hydrometeorology, 16, 1773–1792,

740 https://doi.org/10.1175/JHM-D-15-0019.1, publisher: American Meteorological Society Section: Journal of Hydrometeorology, 2015.

Luthcke, S. B., Thomas, T. C., Pennington, T. A., Rebold, T. W., Nicholas, J. B., Rowlands, D. D., Gardner, A. S., and Bae, S.: ICESat-2 Pointing Calibration and Geolocation Performance, Earth and Space Science, 8, e2020EA001 494, https://doi.org/10.1029/2020EA001494, _eprint: https://onlinelibrary.wiley.com/doi/pdf/10.1029/2020EA001494, 2021.

Magnusson, J., Gustafsson, D., Hüsler, F., and Jonas, T.: Assimilation of point SWE data into a distributed snow cover model

745 comparing two contrasting methods, Water Resources Research, 50, 7816–7835, https://doi.org/10.1002/2014WR015302, _eprint: https://onlinelibrary.wiley.com/doi/pdf/10.1002/2014WR015302, 2014.

Magruder, L., Brunt, K., Neumann, T., Klotz, B., and Alonzo, M.: Passive Ground-Based Optical Techniques for Monitoring the On-Orbit ICESat-2 Altimeter Geolocation and Footprint Diameter, Earth and Space Science, 8, e2020EA001414, https://doi.org/10.1029/2020EA001414, _eprint: https://onlinelibrary.wiley.com/doi/pdf/10.1029/2020EA001414, 2021.

750   Margulis, S. A., Fang, Y., Li, D., Lettenmaier, D. P., and Andreadis, K.: The Utility of Infrequent Snow Depth Images for Deriving Continuous Space-Time Estimates of Seasonal Snow Water Equivalent, Geophysical Research Letters, 46, 5331–5340, https://doi.org/10.1029/2019GL082507, _eprint: https://onlinelibrary.wiley.com/doi/pdf/10.1029/2019GL082507, 2019.

Markus, T., Neumann, T., Martino, A., Abdalati, W., Brunt, K., Csatho, B., Farrell, S., Fricker, H., Gardner, A., Harding, D., Jasinski, M., Kwok, R., Magruder, L., Lubin, D., Luthcke, S., Morison, J., Nelson, R., Neuenschwander, A., Palm, S., Popescu, S., Shum, C., Schutz,

755   B. E., Smith, B., Yang, Y., and Zwally, J.: The Ice, Cloud, and land Elevation Satellite-2 (ICESat-2): Science requirements, concept, and implementation, Remote Sensing of Environment, 190, 260–273, https://doi.org/10.1016/j.rse.2016.12.029, 2017.

Mazzolini, M., Aalstad, K., Alonso-González, E., Westermann, S., and Treichler, D.: Spatio-temporal snow data assimilation with the ICESat-2 laser altimeter, EGUsphere (preprint), https://doi.org/10.5194/egusphere-2024-1404, 2024.

McGill, M. J., Yorks, J. E., Scott, V. S., Kupchock, A. W., and Selmer, P. A.: The Cloud-Aerosol Transport System (CATS): a technology

760   demonstration on the International Space Station, in: Lidar Remote Sensing for Environmental Monitoring XV, vol. 9612, pp. 34–39, SPIE, https://doi.org/10.1117/12.2190841, 2015.

McGrath, C., Lowe, C., Macdonald, M., and Hancock, S.: Investigation of very low Earth orbits (VLEOs) for global spaceborne lidar, CEAS Space J, 14, 625–636, https://doi.org/10.1007/s12567-022-00427-2, 2022.

Meehan, T. G., Hojatimalekshah, A., Marshall, H.-P., Deeb, E. J., O'Neel, S., McGrath, D., Webb, R. W., Bonnell, R., Raleigh, M. S.,

765   Hiemstra, C., and Elder, K.: Spatially distributed snow depth, bulk density, and snow water equivalent from ground-based and airborne sensor integration at Grand Mesa, Colorado, USA, The Cryosphere Discussions, pp. 1–45, https://doi.org/10.5194/tc-2023-141, publisher: Copernicus GmbH, 2023.

Mudryk, L. R., Elias Chereque, A., Derksen, C., Luojus, K., and Decharme, B.: NOAA Arctic Report Card 2023 : Terrestrial Snow Cover, https://doi.org/10.25923/XQWA-H543, publisher: NOAA Global Ocean Monitoring and Observing Program, 2023.

770   Musselman, K. N., Clark, M. P., Liu, C., Ikeda, K., and Rasmussen, R.: Slower snowmelt in a warmer world, Nature Climate Change, 7, 214–219, https://doi.org/10.1038/nclimate3225, publisher: Nature Publishing Group, 2017.

NASEM: Thriving on Our Changing Planet: A Decadal Strategy for Earth Observation from Space, https://doi.org/10.17226/24938, 2018.

Neuenschwander, A. and Pitts, K.: The ATL08 land and vegetation product for the ICESat-2 Mission, Remote Sensing of Environment, 221, 247–259, https://doi.org/10.1016/j.rse.2018.11.005, 2019.

775   Neuenschwander, A., Guenther, E., White, J. C., Duncanson, L., and Montesano, P.: Validation of ICESat-2 terrain and canopy heights in boreal forests, Remote Sensing of Environment, 251, 112110, https://doi.org/10.1016/j.rse.2020.112110, 2020.

Neuenschwander, A. L. and Magruder, L. A.: Canopy and Terrain Height Retrievals with ICESat-2: A First Look, Remote Sensing, 11, 1721, https://doi.org/10.3390/rs11141721, number: 14 Publisher: Multidisciplinary Digital Publishing Institute, 2019.

Neumann, T. A., Martino, A. J., Markus, T., Bae, S., Bock, M. R., Brenner, A. C., Brunt, K. M., Cavanaugh, J., Fernandes, S. T., Han-

780   cock, D. W., Harbeck, K., Lee, J., Kurtz, N. T., Luers, P. J., Luthcke, S. B., Magruder, L., Pennington, T. A., Ramos-Izquierdo, L., Rebold, T., Skoog, J., and Thomas, T. C.: The Ice, Cloud, and Land Elevation Satellite – 2 mission: A global geolocated photon product derived from the Advanced Topographic Laser Altimeter System, Remote Sensing of Environment, 233, 111325, https://doi.org/10.1016/j.rse.2019.111325, 2019.

Nuth, C. and Kääb, A.: Co-registration and bias corrections of satellite elevation data sets for quantifying glacier thickness change, The Cryosphere, 5, 271–290, https://doi.org/10.5194/tc-5-271-2011, publisher: Copernicus GmbH, 2011.

Painter, T. H., Berisford, D. F., Boardman, J. W., Bormann, K. J., Deems, J. S., Gehrke, F., Hedrick, A., Joyce, M., Laidlaw, R., Marks, D., Mattmann, C., McGurk, B., Ramirez, P., Richardson, M., Skiles, S. M., Seidel, F. C., and Winstral, A.: The Airborne Snow Observatory: Fusion of scanning lidar, imaging spectrometer, and physically-based modeling for mapping snow water equivalent and snow albedo, Remote Sensing of Environment, 184, 139–152, https://doi.org/10.1016/j.rse.2016.06.018, 2016.

Palm, S. P., Kayetha, V., Yang, Y., and Pauly, R.: Blowing snow sublimation and transport over Antarctica from 11 years of CALIPSO observations, The Cryosphere, 11, 2555–2569, https://doi.org/10.5194/tc-11-2555-2017, publisher: Copernicus GmbH, 2017.

Pflug, J. M. and Lundquist, J. D.: Inferring Distributed Snow Depth by Leveraging Snow Pattern Repeatability: Investigation Using 47 Lidar Observations in the Tuolumne Watershed, Sierra Nevada, California, Water Resources Research, 56, e2020WR027 243, https://doi.org/10.1029/2020WR027243, _eprint: https://onlinelibrary.wiley.com/doi/pdf/10.1029/2020WR027243, 2020.

Pflug, J. M., Hughes, M., and Lundquist, J. D.: Downscaling Snow Deposition Using Historic Snow Depth Patterns: Diagnosing Limitations From Snowfall Biases, Winter Snow Losses, and Interannual Snow Pattern Repeatability, Water Resources Research, 57, e2021WR029 999, https://doi.org/10.1029/2021WR029999, _eprint: https://onlinelibrary.wiley.com/doi/pdf/10.1029/2021WR029999, 2021.

Pflug, J. M., Margulis, S. A., and Lundquist, J. D.: Inferring watershed-scale mean snowfall magnitude and distribution using multidecadal snow reanalysis patterns and snow pillow observations, Hydrological Processes, 36, e14 581, https://doi.org/10.1002/hyp.14581, _eprint: https://onlinelibrary.wiley.com/doi/pdf/10.1002/hyp.14581, 2022.

Pomeroy, J. W., Gray, D. M., Shook, K. R., Toth, B., Essery, R. L. H., Pietroniro, A., and Hedstrom, N.: An evaluation of snow accumulation and ablation processes for land surface modelling, Hydrological Processes, 12, 2339–2367, https://doi.org/10.1002/(SICI)1099-1085(199812)12:15<2339::AID-HYP800>3.0.CO;2-L, _eprint: https://onlinelibrary.wiley.com/doi/pdf/10.1002/%28SICI%291099-1085%28199812%2912%3A15%3C2339%3A%3AAID-HYP800%3E3.0.CO%3B2-L, 1998.

Popescu, S. C., Zhao, K., Neuenschwander, A., and Lin, C.: Satellite lidar vs. small footprint airborne lidar: Comparing the accuracy of aboveground biomass estimates and forest structure metrics at footprint level, Remote Sensing of Environment, 115, 2786–2797, https://doi.org/10.1016/j.rse.2011.01.026, 2011.

Porter, C., Howat, I., Noh, M.-J., Husby, E., Khuvis, S., Danish, E., Tomko, K., Gardiner, J., Negrete, A., Yadav, B., Klassen, J., Kelleher, C., Cloutier, M., Bakker, J., Enos, J., Arnold, G., Bauer, G., and Morin, P.: ArcticDEM - Mosaics, Version 4.1, https://doi.org/10.7910/DVN/3VDC4W, 2023.

Prokop, A.: Assessing the applicability of terrestrial laser scanning for spatial snow depth measurements, Cold Regions Science and Technology, 54, 155–163, https://doi.org/10.1016/j.coldregions.2008.07.002, 2008.

Raleigh, M. S. and Small, E. E.: Snowpack density modeling is the primary source of uncertainty when mapping basin-wide SWE with lidar, Geophysical Research Letters, 44, 3700–3709, https://doi.org/https://doi.org/10.1002/2016GL071999, 2017.

Raleigh, M. S., Lundquist, J. D., and Clark, M. P.: Exploring the impact of forcing error characteristics on physically based snow simulations within a global sensitivity analysis framework, Hydrology and Earth System Sciences, 19, 3153–3179, https://doi.org/10.5194/hess-19-3153-2015, publisher: Copernicus GmbH, 2015.

Reinking, A. K., Højlund Pedersen, S., Elder, K., Boelman, N. T., Glass, T. W., Oates, B. A., Bergen, S., Roberts, S., Prugh, L. R., Brinkman, T. J., Coughenour, M. B., Feltner, J. A., Barker, K. J., Bentzen, T. W., Pedersen, Ø., Schmidt, N. M., and Liston, G. E.:

Collaborative wildlife–snow science: Integrating wildlife and snow expertise to improve research and management, Ecosphere, 13, e4094, https://doi.org/10.1002/ecs2.4094, 2022.

Revuelto, J., López-Moreno, J. I., Azorin-Molina, C., and Vicente-Serrano, S. M.: Canopy influence on snow depth distribution in a pine stand determined from terrestrial laser data, Water Resources Research, 51, 3476–3489, https://doi.org/10.1002/2014WR016496, _eprint: https://onlinelibrary.wiley.com/doi/pdf/10.1002/2014WR016496, 2015.

Riggs, G. A., Hall, D. K., and Román, M. O.: Overview of NASA's MODIS and Visible Infrared Imaging Radiometer Suite (VIIRS) snow-cover Earth System Data Records, Earth System Science Data, 9, 765–777, https://doi.org/10.5194/essd-9-765-2017, publisher: Copernicus GmbH, 2017.

Scheick, J., Leong, W. J., Bisson, K., Arendt, A., Bhushan, S., Fair, Z., Hagen, N. R., Henderson, S., Knuth, F., Li, T., Liu, Z., Piunno, R., Ravinder, N., Landung, Sutterley, T., Swinski, J., and Anubhav: icepyx: querying, obtaining, analyzing, and manipulating ICESat-2 datasets, Journal of Open Source Software, 8, 4912, https://doi.org/10.21105/joss.04912, 2023.

Schirmer, M. and Lehning, M.: Persistence in intra-annual snow depth distribution: 2. Fractal analysis of snow depth development, Water Resources Research, 47, https://doi.org/10.1029/2010WR009429, _eprint: https://onlinelibrary.wiley.com/doi/pdf/10.1029/2010WR009429, 2011.

Schirmer, M., Wirz, V., Clifton, A., and Lehning, M.: Persistence in intra-annual snow depth distribution: 1. Measurements and topographic control, Water Resources Research, 47, https://doi.org/10.1029/2010WR009426, _eprint: https://onlinelibrary.wiley.com/doi/pdf/10.1029/2010WR009426, 2011.

Schutz, B. E., Zwally, H. J., Shuman, C. A., Hancock, D., and DiMarzio, J. P.: Overview of the ICESat Mission, Geophysical Research Letters, 32, https://doi.org/10.1029/2005GL024009, _eprint: https://onlinelibrary.wiley.com/doi/pdf/10.1029/2005GL024009, 2005.

Shean, D., Bhushan, S., Smith, B., Besso, H., Sutterley, T., Swinski, J.-P., Henderson, S., Neumann, T., and Williams, J. B.: Evaluating and improving seasonal snow depth retrievals with satellite laser altimetry, 2021, C33B–04, https://ui.adsabs.harvard.edu/abs/2021AGUFM.C33B..04S, conference Name: AGU Fall Meeting Abstracts ADS Bibcode: 2021AGUFM.C33B..04S, 2021.

Shean, D., Swinski, J. p., Smith, B., Sutterley, T., Henderson, S., Ugarte, C., Lidwa, E., and Neumann, T.: SlideRule: Enabling rapid, scalable, open science for the NASA ICESat-2 mission and beyond, Journal of Open Source Software, 8, 4982, https://doi.org/10.21105/joss.04982, 2023.

Simpson, J. E., Smith, T. E. L., and Wooster, M. J.: Assessment of Errors Caused by Forest Vegetation Structure in Airborne LiDAR-Derived DTMs, Remote Sensing, 9, 1101, https://doi.org/10.3390/rs9111101, number: 11 Publisher: Multidisciplinary Digital Publishing Institute, 2017.

Smith, B., Fricker, H. A., Holschuh, N., Gardner, A. S., Adusumilli, S., Brunt, K. M., Csatho, B., Harbeck, K., Huth, A., Neumann, T., Nilsson, J., and Siegfried, M. R.: Land ice height-retrieval algorithm for NASA's ICESat-2 photon-counting laser altimeter, Remote Sensing of Environment, 233, 111 352, https://doi.org/10.1016/j.rse.2019.111352, 2019.

Smith, B. E., Gardner, A., Schneider, A., and Flanner, M.: Modeling biases in laser-altimetry measurements caused by scattering of green light in snow, Remote Sensing of Environment, 215, 398–410, https://doi.org/10.1016/j.rse.2018.06.012, 2018.

Smyth, E. J., Raleigh, M. S., and Small, E. E.: Particle Filter Data Assimilation of Monthly Snow Depth Observations Improves Estimation of Snow Density and SWE, Water Resources Research, 55, 1296–1311, https://doi.org/10.1029/2018WR023400, _eprint: https://onlinelibrary.wiley.com/doi/pdf/10.1029/2018WR023400, 2019.

Smyth, E. J., Raleigh, M. S., and Small, E. E.: Improving SWE Estimation With Data Assimilation: The Influence of Snow Depth Observation Timing and Uncertainty, Water Resources Research, 56, e2019WR026 853, https://doi.org/10.1029/2019WR026853, _eprint: https://onlinelibrary.wiley.com/doi/pdf/10.1029/2019WR026853, 2020.

860   Spaete, L. P., Glenn, N. F., Derryberry, D. R., Sankey, T. T., Mitchell, J. J., and Hardegree, S. P.: Vegetation and slope effects on accuracy of a LiDAR-derived DEM in the sagebrush steppe, Remote Sensing Letters, 2, 317–326, https://doi.org/10.1080/01431161.2010.515267, publisher: Taylor & Francis, 2011.

Stoker, J. and Miller, B.: The Accuracy and Consistency of 3D Elevation Program Data: A Systematic Analysis, Remote Sensing, 14, 940, https://doi.org/10.3390/rs14040940, number: 4 Publisher: Multidisciplinary Digital Publishing Institute, 2022.

865   Sturm, M. and Wagner, A. M.: Using repeated patterns in snow distribution modeling: An Arctic example, Water Resources Research, 46, https://doi.org/10.1029/2010WR009434, _eprint: https://onlinelibrary.wiley.com/doi/pdf/10.1029/2010WR009434, 2010.

Sturm, M., Taras, B., Liston, G. E., Derksen, C., Jonas, T., and Lea, J.: Estimating Snow Water Equivalent Using Snow Depth Data and Climate Classes, Journal of Hydrometeorology, 11, 1380–1394, https://doi.org/10.1175/2010JHM1202.1, publisher: American Meteorological Society Section: Journal of Hydrometeorology, 2010.

870   Sutterley, T. C. and Gibbons, A.: pyYAPC: Python interpretation of the NASA Goddard Space Flight Center YAPC ("Yet Another Photon Classifier") algorithm, https://doi.org/10.5281/zenodo.6717591, 2021.

Treichler, D. and Kääb, A.: Snow depth from ICESat laser altimetry — A test study in southern Norway, Remote Sensing of Environment, 191, 389–401, https://doi.org/10.1016/j.rse.2017.01.022, 2017.

Vuyovich, C., Stuefer, S., Durand, M., Marshall, H. P., Osmanoglu, B., Elder, K., Vas, D., Gelvin, A., Larsen, C. F., Pedersen, S.,
875   Hodkinson, D., Deeb, E., Mason, M., and Youcha, E.: NASA SnowEx 2023 Experiment Plan, https://drive.google.com/file/d/1Ev_3JB-BDQ6K5R-YRz0iJr-UdbdcW_OS/view, 2022.

Wang, C., Zhu, X., Nie, S., Xi, X., Li, D., Zheng, W., and Chen, S.: Ground elevation accuracy verification of ICESat-2 data: a case study in Alaska, USA, Opt. Express, OE, 27, 38 168–38 179, https://doi.org/10.1364/OE.27.038168, publisher: Optica Publishing Group, 2019.

Wayand, N. E., Massmann, A., Butler, C., Keenan, E., Stimberis, J., and Lundquist, J. D.: A meteorological and snow obser-
880   vational data set from Snoqualmie Pass (921 m), Washington Cascades, USA, Water Resources Research, 51, 10 092–10 103, https://doi.org/10.1002/2015WR017773, _eprint: https://onlinelibrary.wiley.com/doi/pdf/10.1002/2015WR017773, 2015.

Webb, R. W., Jennings, K. S., Fend, M., and Molotch, N. P.: Combining Ground-Penetrating Radar With Terrestrial LiDAR Scanning to Estimate the Spatial Distribution of Liquid Water Content in Seasonal Snowpacks, Water Resources Research, 54, 10,339–10,349, https://doi.org/10.1029/2018WR022680, _eprint: https://onlinelibrary.wiley.com/doi/pdf/10.1029/2018WR022680, 2018.

885   Winker, D. M., Vaughan, M. A., Omar, A., Hu, Y., Powell, K. A., Liu, Z., Hunt, W. H., and Young, S. A.: Overview of the CALIPSO Mission and CALIOP Data Processing Algorithms, Journal of Atmospheric and Oceanic Technology, 26, 2310–2323, https://doi.org/10.1175/2009JTECHA1281.1, publisher: American Meteorological Society Section: Journal of Atmospheric and Oceanic Technology, 2009.

Wrzesien, M. L., Pavelsky, T. M., Durand, M. T., Dozier, J., and Lundquist, J. D.: Characterizing Biases in Mountain Snow Ac-
890   cumulation From Global Data Sets, Water Resources Research, 55, 9873–9891, https://doi.org/10.1029/2019WR025350, _eprint: https://onlinelibrary.wiley.com/doi/pdf/10.1029/2019WR025350, 2019.

Table 2. List of published studies that used spaceborne lidar for snow depth measurements, with the primary study locations and areal coverage (in km^2), land cover types, and snow depth retrieval method given. The lidar product refers to the spaceborne lidar altimeter of interest, and the reference elevation(s) are the DEMs used for differencing. Hu et al. (2022b) and Lu et al. (2022) have continental-scale study domains, so their areal coverage is not given.

Study	Domain	Land cover	Method	Lidar product	Reference elevation	Validation
Treichler and Kääb (2017)	Hardangervidda, Norway (4500 km^2)	Mountain	Altimetry-DEM differencing	ICESat (GLAH14)	SRTM DEM (45 m) Kartverket DEM (10 m)	Weather stations Airborne lidar DEMs (1 m)
Shean et al. (2021)	Grand Mesa, CO (1300 km^2)	Forest Mountain	Altimetry-DEM differencing	ICESat-2 (ATL08, Sliderule) GEDI (L2A)	Worldview-3 (1 m) 3DEP (1 m) ASO (3 m)	Weather stations
Hu et al. (2022b)	Northern Xinjiang	Bare earth Grassland	Cross-track differencing	ICESat-2 (ATL08)	—	Weather stations
Lu et al. (2022)	Western U.S.	Forest Mountain	Backscatter deconvolution	ICESat-2 (ATL03)	—	4 km reanalysis 24 km reanalysis
Enderlin et al. (2022)	Reynolds Creek, ID (239 km^2) Wolverine Glacier, AK (15.6 km^2)	Mountain glacier Forest	Altimetry-DEM differencing	ICESat-2 (ATL06, ATL08)	Airborne lidar (0.5 m, 1 m) Worldview (2 m)	—
Deschamps-Berger et al. (2023)	Tuolumne Basin, CA (5000 km^2)	Forest Mountain	Altimetry-DEM differencing	ICESat-2 (ATL06)	ASO (15 m) Pléiades (15 m) Copernicus (30 m)	ASO (3-15 m)
Besso et al. (2024)	Tuolumne Basin, CA (5000 km^2) Methow Valley, WA (1800 km^2)	Forest Mountain	Altimetry-DEM differencing	ICESat-2 (SlideRule)	ASO (3 m) Airborne lidar (1 m)	ASO (3 m) Weather stations
?	Hardangervidda, Norway (4500 km^2)	Mountain	Altimetry-DEM differencing	ICESat-2 (ATL03)	Kartverket DEM (10 m)	Sentinel-1 (500 m) In-situ data

Study	Altimeter	Bias metric	Bias (cm)	% of Median Depth	Uncertainty metric	Uncertainty (cm)
Treichler and Kääb (2017)	ICESat	RMSE	9-15 (Western forest) 40-64 (Eastern forest)	5%-8% 34%-55%	NMAD	103
Shean et al. (2021)	GEDI ICESat-2	RMSE	101 19	—	—	—
Hu et al. (2022a)	ICESat-2	RMSE	4.2	27.6%	—	—
Lu et al. (2022)	ICESat-2	RMSE	14	28%	Standard deviation	9.6
Enderlin et al. (2022)	ICESat-2	Residual difference	+20 (slope<0.5°) -100 (slope>20°)	29%	MAD	60
Deschamps-Berger et al. (2023)	ICESat-2	Residual difference	-35 (ASO, slope<10°) +59 (ASO, slope>40°) -53 (Pléiades) +53 (Copernicus)	12% 20% 18% 18%	NMAD	+39 (ASO, slope<10°) +148 (ASO, slope>40°) +84 (Pléiades) +300 (Copernicus)
Besso et al. (2024)	ICESat-2	Residual difference	-5 (slope<10°) -60 (slope>25°)	—	Standard deviation	41

Table 3. Bias and uncertainties for snow depths derived from the studies in Table 2. The accuracy metrics and lidar altimeters for each study are also given. Hu et al. (2022b) is omitted from the table because accuracy and uncertainty of the method is given by Lu et al. (2022).

Error Source	Impact to Lidar	Expected Biases (cm)
Terrain characteristics	Complex topography (surface roughness, slope) makes precise geolocation of the return signal difficult.	> 100 (ATL06/ATL08) 60 (ATL06-SR) for slope > 20°
DEM accuracy and co-registration	Reprojecting to match reference DEMs can cause geolocation uncertainties.	< 10 (lidar DEMs) > 100 (coarse DEMs)
Vegetation	Dense vegetation canopies weaken the return signal. Undergrowth introduces uncertainties in snow-free DEMs.	~ 60 (forest cover $\sim 60\%$) ~ 100 (heavy undergrowth)*
Lidar penetration in snow	The lidar signal experiences scattering within a snowpack, increasing the time it takes to return to the detector.	≤ 10 (Greenland firn)

Table 4. A summary of the error sources discussed in Section 6. The given biases in the right column represent maximum biases reported in available literature. Because undergrowth (*) has not been formally assessed for DEM generation, the given value is speculative from the literature.

Snow variable	DS Requirement	GCOS Requirement	Does spaceborne lidar fulfill objective?	Comments
Snow depth	—	5 km resolution 1 day revisit time 25 mm uncertainty	Yes No Yes	Accuracy is possible over flat terrain. Other environments have decimeter accuracy. Revisit time is not achievable.
Snow cover	1-10 km resolution 1-2 times per day	500 m resolution 1-4 times per day	Needs research	Snow cover metrics have been proposed, but not developed. Optical imagery is preferred.
SWE	4 km resolution 100 m resolution (mountains) 3-5 day revisit time 10-20% accuracy	5 km resolution — 1 day revisit time 30% accuracy (mountains)	Yes Yes No Yes	Gives snow depth, needs density observations or models to derive SWE. Resolution is along-track; across-track is coarser.
Optical properties	30 m resolution	N/A	Needs research	Optical property retrievals have been proposed but not developed.

Table 5. A summary of recommended specifications for four snow variables, and the feasibility of spaceborne lidar to fulfill these requirements from the 2017 Decadal Survey (DS) and Global Climate Observing System (GCOS). Requirements that have the potential to be fulfilled, but do not have published literature relevant to spaceborne lidar, are marked as "Needs research". Caveats for each snow variable are given in the "Comments" column. The GCOS requirements (*) are in the process of being updated, so the values here are subject to change.